CHAPTER

12

COMPRESSIBLE FLOW

For the most part, we have limited our consideration so far to flows for which density variations and thus compressibility effects are negligible. In this chapter, we lift this limitation and consider flows that involve significant changes in density. Such flows are called *compressible flows,* and they are frequently encountered in devices that involve the flow of gases at very high speeds. Compressible flow combines fluid dynamics and thermodynamics in that both are necessary to the development of the required theoretical background. In this chapter, we develop the general relations associated with compressible flows for an ideal gas with constant specific heats.

We start this chapter by reviewing the concepts of *stagnation state, speed of sound,* and *Mach number* for compressible flows. The relationships between the static and stagnation fluid properties are developed for isentropic flows of ideal gases, and they are expressed as functions of specific heat ratios and the Mach number. The effects of area changes for one-dimensional isentropic subsonic and supersonic flows are discussed. These effects are illustrated by considering the isentropic flow through *converging* and *converging–diverging nozzles.* The concept of *shock waves* and the variation of flow properties across normal and oblique shock waves are discussed. Finally, we consider the effects of friction and heat transfer on compressible flows and develop relations for property changes.

OBJECTIVES

When you finish reading this chapter, you should be able to

- Appreciate the consequences of compressibility in gas flow
- Understand why a nozzle must have a diverging section to accelerate a gas to supersonic speeds
- Predict the occurrence of shocks and calculate property changes across a shock wave
- Understand the effects of friction and heat transfer on compressible flows

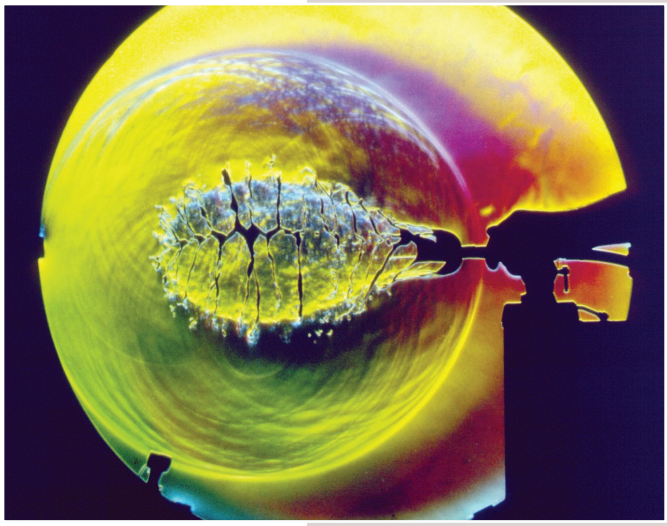

High-speed color schlieren image of the bursting of a toy balloon overfilled with compressed air. This 1-microsecond exposure captures the shattered balloon skin and reveals the bubble of compressed air inside beginning to expand. The balloon burst also drives a weak spherical shock wave, visible here as a circle surrounding the balloon. The silhouette of the photographer's hand on the air valve can be seen at center right.

(*a*)

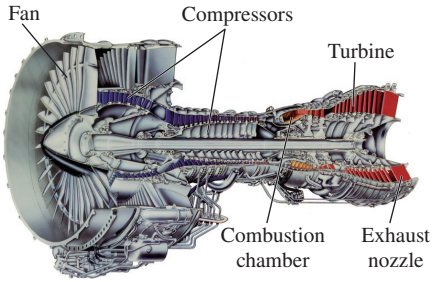

(*b*)

FIGURE 12–1
Aircraft and jet engines involve high speeds, and thus the kinetic energy term should always be considered when analyzing them.

(a) © Corbis RF; (b) Photo courtesy of United Technologies Corporation/Pratt & Whitney. Used by permission. All rights reserved.

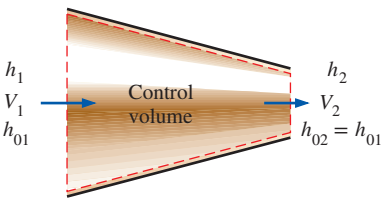

FIGURE 12–2
Steady flow of a fluid through an adiabatic duct.

12–1 ▪ STAGNATION PROPERTIES

When analyzing control volumes, we find it very convenient to combine the *internal energy* and the *flow energy* of a fluid into a single term, *enthalpy,* defined per unit mass as $h = u + P/\rho$. Whenever the kinetic and potential energies of the fluid are negligible, as is often the case, the enthalpy represents the *total energy* of a fluid. For high-speed flows, such as those encountered in jet engines (Fig. 12–1), the potential energy of the fluid is still negligible, but the kinetic energy is not. In such cases, it is convenient to combine the enthalpy and the kinetic energy of the fluid into a single term called **stagnation** (or **total**) **enthalpy** h_0, defined per unit mass as

$$h_0 = h + \frac{V^2}{2} \quad \text{(kJ/kg)} \tag{12–1}$$

When the potential energy of the fluid is negligible, the stagnation enthalpy represents the *total energy of a flowing fluid stream* per unit mass. Thus it simplifies the thermodynamic analysis of high-speed flows.

Throughout this chapter the ordinary enthalpy h is referred to as the **static enthalpy**, whenever necessary, to distinguish it from the stagnation enthalpy. Notice that the stagnation enthalpy is a combination property of a fluid, just like the static enthalpy, and these two enthalpies are identical when the kinetic energy of the fluid is negligible.

Consider the steady flow of a fluid through a duct such as a nozzle, diffuser, or some other flow passage where the flow takes place adiabatically and with no shaft or electrical work, as shown in Fig. 12–2. Assuming the fluid experiences little or no change in its elevation and its potential energy, the energy balance relation ($\dot{E}_{\text{in}} = \dot{E}_{\text{out}}$) for this single-stream steady-flow device reduces to

$$h_1 + \frac{V_1^2}{2} = h_2 + \frac{V_2^2}{2} \tag{12–2}$$

or

$$h_{01} = h_{02} \tag{12–3}$$

That is, in the absence of any heat and work interactions and any changes in potential energy, the stagnation enthalpy of a fluid remains constant during a steady-flow process. Flows through nozzles and diffusers usually satisfy these conditions, and any increase in fluid velocity in these devices creates an equivalent decrease in the static enthalpy of the fluid.

If the fluid were brought to a complete stop, then the velocity at state 2 would be zero and Eq. 12–2 would become

$$h_1 + \frac{V_1^2}{2} = h_2 = h_{02}$$

Thus the *stagnation enthalpy* represents the *enthalpy of a fluid when it is brought to rest adiabatically.*

During a stagnation process, the kinetic energy of a fluid is converted to enthalpy (internal energy + flow energy), which results in an increase in the fluid temperature and pressure. The properties of a fluid at the stagnation state are called **stagnation properties** (stagnation temperature, stagnation

pressure, stagnation density, etc.). The stagnation state and the stagnation properties are indicated by the subscript 0.

The stagnation state is called the **isentropic stagnation state** when the stagnation process is reversible as well as adiabatic (i.e., isentropic). The entropy of a fluid remains constant during an isentropic stagnation process. The actual (irreversible) and isentropic stagnation processes are shown on an *h-s* diagram in Fig. 12–3. Notice that the stagnation enthalpy of the fluid (and the stagnation temperature if the fluid is an ideal gas) is the same for both cases. However, the actual stagnation pressure is lower than the isentropic stagnation pressure since entropy increases during the actual stagnation process as a result of fluid friction. Many stagnation processes are approximated to be isentropic, and isentropic stagnation properties are simply referred to as stagnation properties.

When the fluid is approximated as an *ideal gas* with constant specific heats, its enthalpy can be replaced by c_pT and Eq. 12–1 is expressed as

$$c_pT_0 = c_pT + \frac{V^2}{2}$$

or

$$T_0 = T + \frac{V^2}{2c_p} \tag{12–4}$$

Here, T_0 is called the **stagnation** (or **total**) **temperature**, and it represents *the temperature an ideal gas attains when it is brought to rest adiabatically.* The term $V^2/2c_p$ corresponds to the temperature rise during such a process and is called the **dynamic temperature**. For example, the dynamic temperature of air flowing at 100 m/s is $(100\ \text{m/s})^2/(2 \times 1.005\ \text{kJ/kg·K}) = 5.0\ \text{K}$. Therefore, when air at 300 K and 100 m/s is brought to rest adiabatically (at the tip of a temperature probe, for example), its temperature rises to the stagnation value of 305 K (Fig. 12–4). Note that for low-speed flows, the stagnation and static (or ordinary) temperatures are practically the same. But for high-speed flows, the temperature measured by a stationary probe placed in the fluid (the stagnation temperature) may be significantly higher than the static temperature of the fluid.

The pressure a fluid attains when brought to rest isentropically is called the **stagnation pressure** P_0. For ideal gases with constant specific heats, P_0 is related to the static pressure of the fluid by

$$\frac{P_0}{P} = \left(\frac{T_0}{T}\right)^{k/(k-1)} \tag{12–5}$$

By noting that $\rho = 1/\upsilon$ and using the isentropic relation $P\upsilon^k = P_0\upsilon_0^k$, the ratio of the stagnation density to static density is expressed as

$$\frac{\rho_0}{\rho} = \left(\frac{T_0}{T}\right)^{1/(k-1)} \tag{12–6}$$

When stagnation enthalpies are used, there is no need to refer explicitly to kinetic energy. Then the energy balance $\dot{E}_{\text{in}} = \dot{E}_{\text{out}}$ for a single-stream, steady-flow device can be expressed as

$$q_{\text{in}} + w_{\text{in}} + (h_{01} + gz_1) = q_{\text{out}} + w_{\text{out}} + (h_{02} + gz_2) \tag{12–7}$$

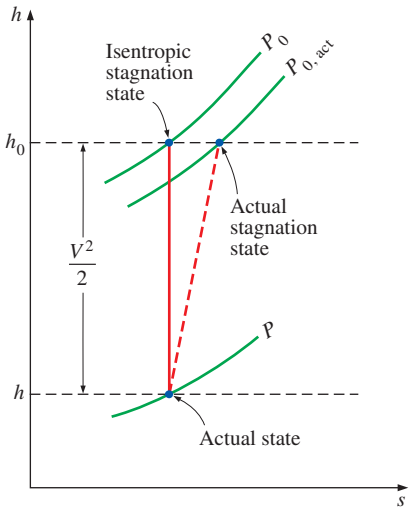

FIGURE 12–3
The actual state, actual stagnation state, and isentropic stagnation state of a fluid on an *h-s* diagram.

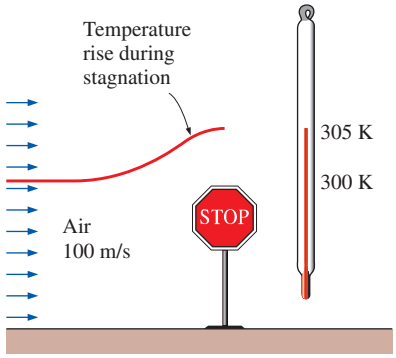

FIGURE 12–4
The temperature of an ideal gas flowing at a velocity V rises by $V^2/2c_p$ when it is brought to a complete stop.

where h_{01} and h_{02} are the stagnation enthalpies at states 1 and 2, respectively. When the fluid is an ideal gas with constant specific heats, Eq. 12–7 becomes

$$(q_{in} - q_{out}) + (w_{in} - w_{out}) = c_p(T_{02} - T_{01}) + g(z_2 - z_1) \quad \textbf{(12–8)}$$

where T_{01} and T_{02} are the stagnation temperatures.

Notice that kinetic energy terms do not explicitly appear in Eqs. 12–7 and 12–8, but the stagnation enthalpy terms account for their contribution.

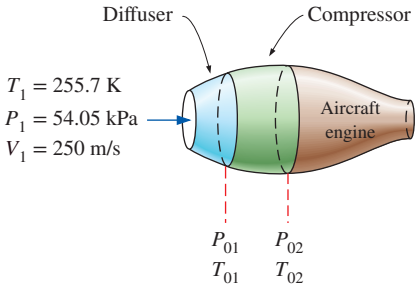

FIGURE 12–5
Schematic for Example 12–1.

EXAMPLE 12–1 Compression of High-Speed Air in an Aircraft

An aircraft is flying at a cruising speed of 250 m/s at an altitude of 5000 m where the atmospheric pressure is 54.05 kPa and the ambient air temperature is 255.7 K. The ambient air is first decelerated in a diffuser before it enters the compressor (Fig. 12–5). Approximating both the diffuser and the compressor to be isentropic, determine (*a*) the stagnation pressure at the compressor inlet and (*b*) the required compressor work per unit mass if the stagnation pressure ratio of the compressor is 8.

SOLUTION High-speed air enters the diffuser and the compressor of an aircraft. The stagnation pressure of the air and the compressor work input are to be determined.

Assumptions **1** Both the diffuser and the compressor are isentropic. **2** Air is an ideal gas with constant specific heats at room temperature.

Properties The constant-pressure specific heat c_p and the specific heat ratio k of air at room temperature are

$$c_p = 1.005 \text{ kJ/kg·K} \quad \text{and} \quad k = 1.4$$

Analysis (*a*) Under isentropic conditions, the stagnation pressure at the compressor inlet (diffuser exit) can be determined from Eq. 12–5. However, first we need to find the stagnation temperature T_{01} at the compressor inlet. Under the stated assumptions, T_{01} is determined from Eq. 12–4 to be

$$T_{01} = T_1 + \frac{V_1^2}{2c_p} = 255.7 \text{ K} + \frac{(250 \text{ m/s})^2}{(2)(1.005 \text{ kJ/kg·K})}\left(\frac{1 \text{ kJ/kg}}{1000 \text{ m}^2/\text{s}^2}\right)$$
$$= 286.8 \text{ K}$$

Then from Eq. 12–5,

$$P_{01} = P_1\left(\frac{T_{01}}{T_1}\right)^{k/(k-1)} = (54.05 \text{ kPa})\left(\frac{286.8 \text{ K}}{255.7 \text{ K}}\right)^{1.4/(1.4-1)}$$
$$= \mathbf{80.77 \text{ kPa}}$$

That is, the temperature of air would increase by 31.1°C and the pressure by 26.72 kPa as air is decelerated from 250 m/s to zero velocity. These increases in the temperature and pressure of air are due to the conversion of the kinetic energy into enthalpy.

(*b*) To determine the compressor work, we need to know the stagnation temperature of air at the compressor exit T_{02}. The stagnation pressure ratio across the compressor P_{02}/P_{01} is specified to be 8. Since the compression process is approximated as isentropic, T_{02} can be determined from the ideal-gas isentropic relation (Eq. 12–5):

$$T_{02} = T_{01}\left(\frac{P_{02}}{P_{01}}\right)^{(k-1)/k} = (286.8 \text{ K})(8)^{(1.4-1)/1.4} = 519.5 \text{ K}$$

Disregarding potential energy changes and heat transfer, the compressor work per unit mass of air is determined from Eq. 12–8:

$$\begin{aligned} w_{\text{in}} &= c_p(T_{02} - T_{01}) \\ &= (1.005\ \text{kJ/kg·K})(519.5\ \text{K} - 286.8\ \text{K}) \\ &= \mathbf{233.9\ kJ/kg} \end{aligned}$$

Thus the work supplied to the compressor is 233.9 kJ/kg.

Discussion Notice that using stagnation properties automatically accounts for any changes in the kinetic energy of a fluid stream.

12–2 ▪ ONE-DIMENSIONAL ISENTROPIC FLOW

An important parameter in the study of compressible flow is the **speed of sound** c, which was shown in Chap. 2 to be related to other fluid properties as

$$c = \sqrt{(\partial P/\partial \rho)_s} \tag{12–9}$$

or

$$c = \sqrt{k(\partial P/\partial \rho)_T} \tag{12–10}$$

For an ideal gas it simplifies to

$$c = \sqrt{kRT} \tag{12–11}$$

where k is the specific heat ratio of the gas and R is the specific gas constant. The ratio of the speed of the flow to the speed of sound is the dimensionless Mach number Ma,

$$\text{Ma} = \frac{V}{c} \tag{12–12}$$

During fluid flow through many devices such as nozzles, diffusers, and turbine blade passages, flow quantities vary primarily in the flow direction only, and the flow can be approximated as one-dimensional isentropic flow with good accuracy. Therefore, it merits special consideration. Before presenting a formal discussion of one-dimensional isentropic flow, we illustrate some important aspects of it with an example.

EXAMPLE 12–2 Gas Flow through a Converging–Diverging Duct

Carbon dioxide flows steadily through a varying cross-sectional area duct such as a nozzle shown in Fig. 12–6 at a mass flow rate of 3.00 kg/s. The carbon dioxide enters the duct at a pressure of 1400 kPa and 200°C with a low velocity, and it expands in the nozzle to an exit pressure of 200 kPa. The duct is designed so that the flow can be approximated as isentropic. Determine the density, velocity, flow area, and Mach number at each location along the duct that corresponds to an overall pressure drop of 200 kPa.

SOLUTION Carbon dioxide enters a varying cross-sectional area duct at specified conditions. The flow properties are to be determined along the duct.

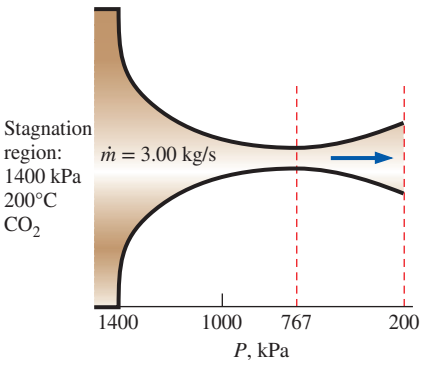

FIGURE 12–6
Schematic for Example 12–2.

Assumptions **1** Carbon dioxide is an ideal gas with constant specific heats at room temperature. **2** Flow through the duct is steady, one-dimensional, and isentropic.

Properties For simplicity we use $c_p = 0.846$ kJ/kg·K and $k = 1.289$ throughout the calculations, which are the constant-pressure specific heat and specific heat ratio values of carbon dioxide at room temperature. The gas constant of carbon dioxide is $R = 0.1889$ kJ/kg·K.

Analysis We note that the inlet temperature is nearly equal to the stagnation temperature since the inlet velocity is small. The flow is isentropic, and thus the stagnation temperature and pressure throughout the duct remain constant. Therefore,

$$T_0 \cong T_1 = 200°\text{C} = 473\ \text{K}$$

and

$$P_0 \cong P_1 = 1400\ \text{kPa}$$

To illustrate the solution procedure, we calculate the desired properties at the location where the pressure is 1200 kPa, the first location that corresponds to a pressure drop of 200 kPa.

From Eq. 12–5,

$$T = T_0\left(\frac{P}{P_0}\right)^{(k-1)/k} = (473\ \text{K})\left(\frac{1200\ \text{kPa}}{1400\ \text{kPa}}\right)^{(1.289-1)/1.289} = 457\ \text{K}$$

From Eq. 12–4,

$$V = \sqrt{2c_p(T_0 - T)}$$

$$= \sqrt{2(0.846\ \text{kJ/kg·K})(473\ \text{K} - 457\ \text{K})\left(\frac{1000\ \text{m}^2/\text{s}^3}{1\ \text{kJ/kg}}\right)}$$

$$= 164.5\ \text{m/s} \cong \mathbf{164\ m/s}$$

From the ideal-gas relation,

$$\rho = \frac{P}{RT} = \frac{1200\ \text{kPa}}{(0.1889\ \text{kPa·m}^3/\text{kg·K})(457\ \text{K})} = \mathbf{13.9\ kg/m^3}$$

From the mass flow rate relation,

$$A = \frac{\dot{m}}{\rho V} = \frac{3.00\ \text{kg/s}}{(13.9\ \text{kg/m}^3)(164.5\ \text{m/s})} = 13.1 \times 10^{-4}\ \text{m}^2 = \mathbf{13.1\ cm^2}$$

From Eqs. 12–11 and 12–12,

$$c = \sqrt{kRT} = \sqrt{(1.289)(0.1889\ \text{kJ/kg·K})(457\ \text{K})\left(\frac{1000\ \text{m}^2/\text{s}^2}{1\ \text{kJ/kg}}\right)} = 333.6\ \text{m/s}$$

$$\text{Ma} = \frac{V}{c} = \frac{164.5\ \text{m/s}}{333.6\ \text{m/s}} = \mathbf{0.493}$$

The results for the other pressure steps are summarized in Table 12–1 and are plotted in Fig. 12–7.

Discussion Note that as the pressure decreases, the temperature and speed of sound decrease while the fluid velocity and Mach number increase in the flow direction. The density decreases slowly at first and rapidly later as the fluid velocity increases.

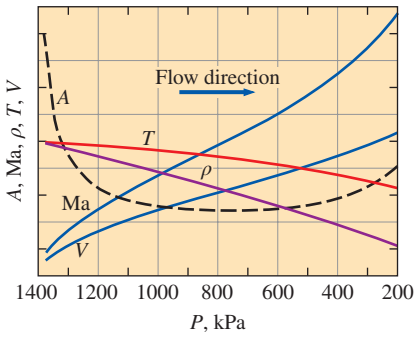

FIGURE 12–7
Variation of normalized fluid properties and cross-sectional area along a duct as the pressure drops from 1400 to 200 kPa.

TABLE 12–1

Variation of fluid properties in flow direction in the duct described in Example 12–2 for $\dot{m} = 3$ kg/s = constant

P, kPa	T, K	V, m/s	ρ, kg/m^3	c, m/s	A, cm^2	Ma
1400	473	0	15.7	339.4	∞	0
1200	457	164.5	13.9	333.6	13.1	0.493
1000	439	240.7	12.1	326.9	10.3	0.736
800	417	306.6	10.1	318.8	9.64	0.962
767*	413	317.2	9.82	317.2	9.63	1.000
600	391	371.4	8.12	308.7	10.0	1.203
400	357	441.9	5.93	295.0	11.5	1.498
200	306	530.9	3.46	272.9	16.3	1.946

* 767 kPa is the critical pressure where the local Mach number is unity.

We note from Example 12–2 that the flow area decreases with decreasing pressure down to a critical-pressure value where the Mach number is unity, and then it begins to increase with further reductions in pressure. The Mach number is unity at the location of smallest flow area, called the **throat** (Fig. 12–8). Note that the velocity of the fluid keeps increasing after passing the throat although the flow area increases rapidly in that region. This increase in velocity past the throat is due to the rapid decrease in the fluid density. The flow area of the duct considered in this example first decreases and then increases. Such ducts are called **converging–diverging nozzles**. These nozzles are used to accelerate gases to supersonic speeds and should not be confused with *Venturi nozzles,* which are used strictly for incompressible flow. The first use of such a nozzle occurred in 1893 in a steam turbine designed by a Swedish engineer, Carl G. B. de Laval (1845–1913), and therefore converging–diverging nozzles are often called *Laval nozzles.*

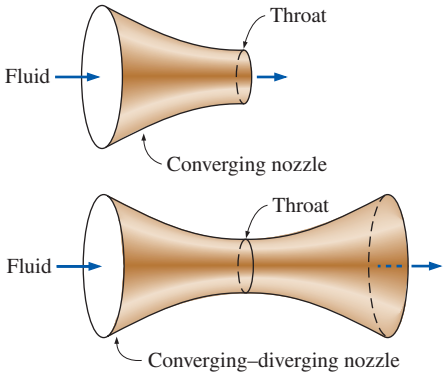

FIGURE 12–8
The cross section of a nozzle at the smallest flow area is called the *throat.*

Variation of Fluid Velocity with Flow Area

It is clear from Example 12–2 that the couplings among the velocity, density, and flow areas for isentropic duct flow are rather complex. In the remainder of this section we investigate these couplings more thoroughly, and we develop relations for the variation of static-to-stagnation property ratios with the Mach number for pressure, temperature, and density.

We begin our investigation by seeking relationships among the pressure, temperature, density, velocity, flow area, and Mach number for one-dimensional isentropic flow. Consider the mass balance for a steady-flow process:

$$\dot{m} = \rho A V = \text{constant}$$

Differentiating and dividing the resultant equation by the mass flow rate, we obtain

$$\frac{d\rho}{\rho} + \frac{dA}{A} + \frac{dV}{V} = 0 \qquad \textbf{(12–13)}$$

Neglecting the potential energy, the energy balance for an isentropic flow with no work interactions is expressed in differential form as (Fig. 12–9)

$$\frac{dP}{\rho} + V\,dV = 0 \qquad \textbf{(12–14)}$$

CONSERVATION OF ENERGY
(steady flow, $w = 0$, $q = 0$, $\Delta pe = 0$)

$$h_1 + \frac{V_1^2}{2} = h_2 + \frac{V_2^2}{2}$$

or

$$h + \frac{V^2}{2} = \text{constant}$$

Differentiate,

$$dh + V\,dV = 0$$

Also,

$$T\,ds = dh - v\,dP \quad (0 \text{ (isentropic)})$$

$$dh = v\,dP = \frac{1}{\rho}\,dP$$

Substitute,

$$\frac{dP}{\rho} + V\,dV = 0$$

FIGURE 12–9
Derivation of the differential form of the energy equation for steady isentropic flow.

This relation is also the differential form of Bernoulli's equation when changes in potential energy are negligible, which is a form of Newton's second law of motion for steady-flow control volumes. Combining Eqs. 12–13 and 12–14 gives

$$\frac{dA}{A} = \frac{dP}{\rho}\left(\frac{1}{V^2} - \frac{d\rho}{dP}\right) \tag{12–15}$$

Rearranging Eq. 12–9 as $(\partial\rho/\partial P)_s = 1/c^2$ and substituting into Eq. 12–15 yield

$$\frac{dA}{A} = \frac{dP}{\rho V^2}(1 - \mathrm{Ma}^2) \tag{12–16}$$

This is an important relation for isentropic flow in ducts since it describes the variation of pressure with flow area. We note that A, ρ, and V are positive quantities. For *subsonic* flow (Ma < 1), the term $1 - \mathrm{Ma}^2$ is positive; and thus dA and dP must have the same sign. That is, the pressure of the fluid must increase as the flow area of the duct increases and must decrease as the flow area of the duct decreases. Thus, at subsonic velocities, the pressure decreases in converging ducts (subsonic nozzles) and increases in diverging ducts (subsonic diffusers).

In *supersonic* flow (Ma > 1), the term $1 - \mathrm{Ma}^2$ is negative, and thus dA and dP must have opposite signs. That is, the pressure of the fluid must increase as the flow area of the duct decreases and must decrease as the flow area of the duct increases. Thus, at supersonic velocities, the pressure decreases in diverging ducts (supersonic nozzles) and increases in converging ducts (supersonic diffusers).

Another important relation for the isentropic flow of a fluid is obtained by substituting $\rho V = -dP/dV$ from Eq. 12–14 into Eq. 12–16:

$$\frac{dA}{A} = -\frac{dV}{V}(1 - \mathrm{Ma}^2) \tag{12–17}$$

This equation governs the shape of a nozzle or a diffuser in subsonic or supersonic isentropic flow. Noting that A and V are positive quantities, we conclude the following:

$$\text{For subsonic flow (Ma} < 1), \quad \frac{dA}{dV} < 0$$

$$\text{For supersonic flow (Ma} > 1), \quad \frac{dA}{dV} > 0$$

$$\text{For sonic flow (Ma} = 1), \quad \frac{dA}{dV} = 0$$

Thus the proper shape of a nozzle depends on the highest velocity desired relative to the sonic velocity. To accelerate a fluid, we must use a converging nozzle at subsonic velocities and a diverging nozzle at supersonic velocities. The velocities encountered in most familiar applications are well below the sonic velocity, and thus it is natural that we visualize a nozzle as a converging duct. However, the highest velocity we can achieve by a converging nozzle is the sonic velocity, which occurs at the exit of the nozzle. If we extend the converging nozzle by further decreasing the flow area, in hopes of accelerating the fluid to supersonic velocities, as shown in Fig. 12–10,

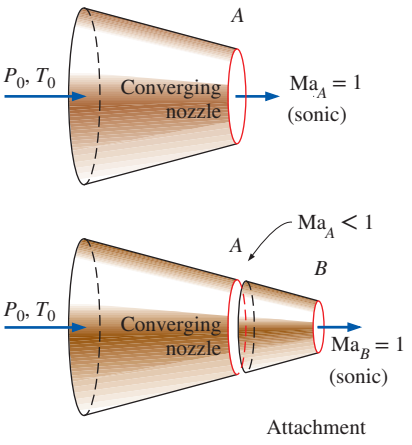

FIGURE 12–10
We cannot attain supersonic velocities by extending the converging section of a converging nozzle. Doing so will only move the sonic cross section farther downstream and decrease the mass flow rate.

we are up for disappointment. Now the sonic velocity will occur at the exit of the converging extension, instead of the exit of the original nozzle, and the mass flow rate through the nozzle will decrease because of the reduced exit area.

Based on Eq. 12–16, which is an expression of the conservation of mass and energy principles, we must add a diverging section to a converging nozzle to accelerate a fluid to supersonic velocities. The result is a converging– diverging nozzle. The fluid first passes through a subsonic (converging) section, where the Mach number increases as the flow area of the nozzle decreases, and then reaches the value of unity at the nozzle throat. The fluid continues to accelerate as it passes through a supersonic (diverging) section. Noting that $\dot{m} = \rho AV$ for steady flow, we see that the large decrease in density makes acceleration in the diverging section possible. An example of this type of flow is the flow of hot combustion gases through a nozzle in a gas turbine.

The opposite process occurs in the engine inlet of a supersonic aircraft. The fluid is decelerated by passing it first through a supersonic diffuser, which has a flow area that decreases in the flow direction. Ideally, the flow reaches a Mach number of unity at the diffuser throat. The fluid is further decelerated in a subsonic diffuser, which has a flow area that increases in the flow direction, as shown in Fig. 12–11.

Property Relations for Isentropic Flow of Ideal Gases

Next we develop relations between the static properties and stagnation properties of an ideal gas in terms of the specific heat ratio k and the Mach number Ma. We assume the flow is isentropic and the gas has constant specific heats.

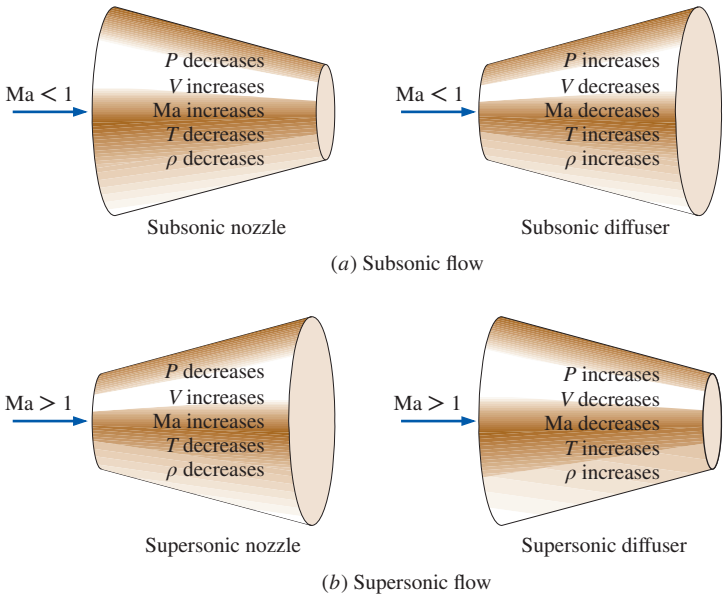

FIGURE 12–11
Variation of flow properties in subsonic and supersonic nozzles and diffusers.

The temperature T of an ideal gas anywhere in the flow is related to the stagnation temperature T_0 through Eq. 12–4:

$$T_0 = T + \frac{V^2}{2c_p}$$

or

$$\frac{T_0}{T} = 1 + \frac{V^2}{2c_pT}$$

Noting that $c_p = kR/(k-1)$, $c^2 = kRT$, and $\text{Ma} = V/c$, we see that

$$\frac{V^2}{2c_pT} = \frac{V^2}{2[kR/(k-1)]T} = \left(\frac{k-1}{2}\right)\frac{V^2}{c^2} = \left(\frac{k-1}{2}\right)\text{Ma}^2$$

Substitution yields

$$\frac{T_0}{T} = 1 + \left(\frac{k-1}{2}\right)\text{Ma}^2 \qquad \textbf{(12–18)}$$

which is the desired relation between T_0 and T.

The ratio of the stagnation to static pressure is obtained by substituting Eq. 12–18 into Eq. 12–5:

$$\frac{P_0}{P} = \left[1 + \left(\frac{k-1}{2}\right)\text{Ma}^2\right]^{k/(k-1)} \qquad \textbf{(12–19)}$$

The ratio of the stagnation to static density is obtained by substituting Eq. 12–18 into Eq. 12–6:

$$\frac{\rho_0}{\rho} = \left[1 + \left(\frac{k-1}{2}\right)\text{Ma}^2\right]^{1/(k-1)} \qquad \textbf{(12–20)}$$

Numerical values of T/T_0, P/P_0, and ρ/ρ_0 are listed versus the Mach number in Table A–13 for $k = 1.4$, which are very useful for practical compressible flow calculations involving air.

The properties of a fluid at a location where the Mach number is unity (the throat) are called **critical properties**, and the ratios in Eqs. (12–18) through (12–20) are called **critical ratios** when Ma = 1 (Fig. 12–12). It is standard practice in the analysis of compressible flow to let the superscript asterisk (*) represent the critical values. Setting Ma = 1 in Eqs. 12–18 through 12–20 yields

$$\frac{T^*}{T} = \frac{2}{k+1} \qquad \textbf{(12–21)}$$

$$\frac{P^*}{P_0} = \left(\frac{2}{k+1}\right)^{k/(k-1)} \qquad \textbf{(12–22)}$$

$$\frac{\rho^*}{\rho_0} = \left(\frac{2}{k+1}\right)^{1/(k-1)} \qquad \textbf{(12–23)}$$

These ratios are evaluated for various values of k and are listed in Table 12–2. The critical properties of compressible flow should not be confused with the thermodynamic properties of substances at the *critical point* (such as the critical temperature T_{cr} and critical pressure P_{cr}).

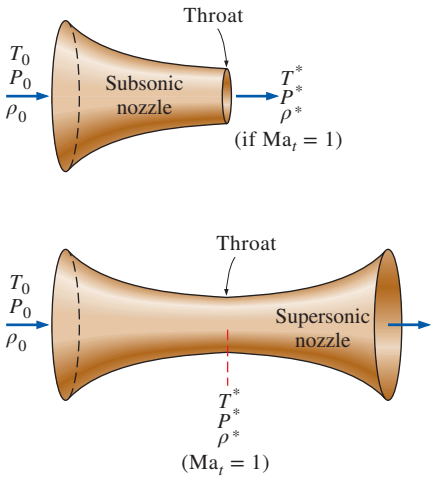

FIGURE 12–12
When $\text{Ma}_t = 1$, the properties at the nozzle throat are the critical properties.

TABLE 12–2

The critical-pressure, critical-temperature, and critical-density ratios for isentropic flow of some ideal gases

	Superheated steam, $k = 1.3$	Hot products of combustion, $k = 1.33$	Air, $k = 1.4$	Monatomic gases, $k = 1.667$
$\frac{P^*}{P_0}$	0.5457	0.5404	0.5283	0.4871
$\frac{T^*}{T_0}$	0.8696	0.8584	0.8333	0.7499
$\frac{\rho^*}{\rho_0}$	0.6276	0.6295	0.6340	0.6495

EXAMPLE 12–3 Critical Temperature and Pressure in Gas Flow

Calculate the critical pressure and temperature of carbon dioxide for the flow conditions described in Example 12–2 (Fig. 12–13).

SOLUTION For the flow discussed in Example 12–2, the critical pressure and temperature are to be calculated.

Assumptions **1** The flow is steady, adiabatic, and one-dimensional. **2** Carbon dioxide is an ideal gas with constant specific heats.

Properties The specific heat ratio of carbon dioxide at room temperature is $k = 1.289$.

Analysis The ratios of critical to stagnation temperature and pressure are determined to be

$$\frac{T^*}{T_0} = \frac{2}{k+1} = \frac{2}{1.289+1} = 0.8737$$

$$\frac{P^*}{P_0} = \left(\frac{2}{k+1}\right)^{k/(k-1)} = \left(\frac{2}{1.289+1}\right)^{1.289/(1.289-1)} = 0.5477$$

Noting that the stagnation temperature and pressure are, from Example 12–2, $T_0 = 473$ K and $P_0 = 1400$ kPa, we see that the critical temperature and pressure in this case are

$$T^* = 0.8737T_0 = (0.8737)(473\ \text{K}) = \mathbf{413\ K}$$

$$P^* = 0.5477P_0 = (0.5477)(1400\ \text{kPa}) = \mathbf{767\ kPa}$$

Discussion Note that these values agree with those listed in the 5th row of Table 12–1, as expected. Also, property values other than these at the throat would indicate that the flow is not critical, and the Mach number is not unity.

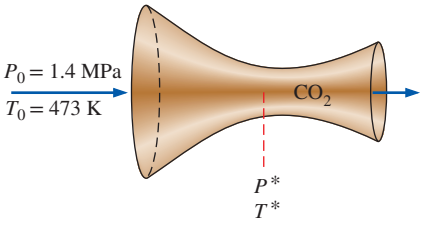

FIGURE 12–13
Schematic for Example 12–3.

12–3 ▪ ISENTROPIC FLOW THROUGH NOZZLES

Converging or converging–diverging nozzles are found in many engineering applications including steam and gas turbines, aircraft and spacecraft propulsion systems, and even industrial blasting nozzles and torch nozzles. In this section we consider the effects of **back pressure** (i.e., the pressure applied

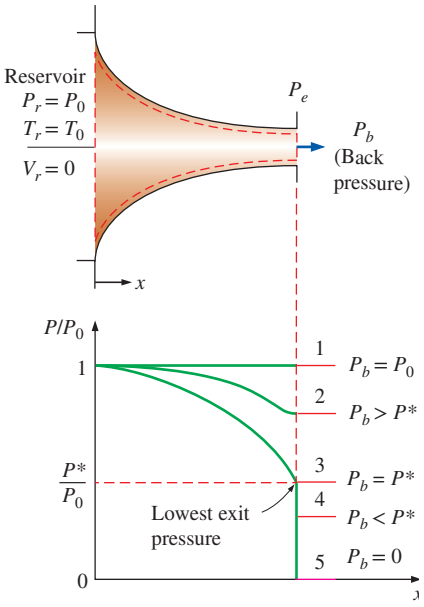

FIGURE 12–14
The effect of back pressure on the pressure distribution along a converging nozzle.

at the nozzle discharge region) on the exit velocity, the mass flow rate, and the pressure distribution along the nozzle.

Converging Nozzles

Consider the subsonic flow through a converging nozzle as shown in Fig. 12–14. The nozzle inlet is attached to a reservoir at pressure P_r and temperature T_r. The reservoir is sufficiently large so that the nozzle inlet velocity is negligible. Since the fluid velocity in the reservoir is zero and the flow through the nozzle is approximated as isentropic, the stagnation pressure and stagnation temperature of the fluid at any cross section through the nozzle are equal to the reservoir pressure and temperature, respectively.

Now we begin to reduce the back pressure and observe the resulting effects on the pressure distribution along the length of the nozzle, as shown in Fig. 12–14. If the back pressure P_b is equal to P_1, which is equal to P_r, there is no flow and the pressure distribution is uniform along the nozzle. When the back pressure is reduced to P_2, the exit plane pressure P_e also drops to P_2. This causes the pressure along the nozzle to decrease in the flow direction.

When the back pressure is reduced to P_3 (= P^*, which is the pressure required to increase the fluid velocity to the speed of sound at the exit plane or throat), the mass flow reaches a maximum value and the flow is said to be **choked**. Further reduction of the back pressure to level P_4 or below does not result in additional changes in the pressure distribution, or anything else along the nozzle length.

Under steady-flow conditions, the mass flow rate through the nozzle is constant and is expressed as

$$\dot{m} = \rho A V = \left(\frac{P}{RT}\right) A(\mathrm{Ma}\sqrt{kRT}) = PA\mathrm{Ma}\sqrt{\frac{k}{RT}}$$

Solving for T from Eq. 12–18 and for P from Eq. 12–19 and substituting,

$$\dot{m} = \frac{A\mathrm{Ma}P_0\sqrt{k/(RT_0)}}{[1 + (k-1)\mathrm{Ma}^2/2]^{(k+1)/[2(k-1)]}} \qquad \textbf{(12–24)}$$

Thus the mass flow rate of a particular fluid through a nozzle is a function of the stagnation properties of the fluid, the flow area, and the Mach number. Equation 12–24 is valid at any cross section, and thus $\dot{m}$ can be evaluated at any location along the length of the nozzle.

For a specified flow area A and stagnation properties T_0 and P_0, the maximum mass flow rate can be determined by differentiating Eq. 12–24 with respect to Ma and setting the result equal to zero. It yields Ma = 1. Since the only location in a nozzle where the Mach number can be unity is the location of minimum flow area (the throat), the mass flow rate through a nozzle is a maximum when Ma = 1 at the throat. Denoting this area by A^*, we obtain an expression for the maximum mass flow rate by substituting Ma = 1 in Eq. 12–24:

$$\dot{m}_{\max} = A^* P_0 \sqrt{\frac{k}{RT_0}} \left(\frac{2}{k+1}\right)^{(k+1)/[2(k-1)]} \qquad \textbf{(12–25)}$$

Thus, for a particular ideal gas, the maximum mass flow rate through a nozzle with a given throat area is fixed by the stagnation pressure and temperature of the inlet flow. The flow rate can be controlled by changing the stagnation pressure or temperature, and thus a converging nozzle can be used as a flowmeter. The flow rate can also be controlled, of course, by varying the throat area. This principle is very important for chemical processes, medical devices, flowmeters, and anywhere the mass flux of a gas must be known and controlled.

A plot of $\dot{m}$ versus P_b/P_0 for a converging nozzle is shown in Fig. 12–15. Notice that the mass flow rate increases with decreasing P_b/P_0, reaches a maximum at $P_b = P^*$, and remains constant for P_b/P_0 values less than this critical ratio. Also illustrated on this figure is the effect of back pressure on the nozzle exit pressure P_e. We observe that

$$P_e = \begin{cases} P_b & \text{for } P_b \geq P^* \\ P^* & \text{for } P_b < P^* \end{cases}$$

To summarize, for all back pressures lower than the critical pressure P^*, the pressure at the exit plane of the converging nozzle P_e is equal to P^*, the Mach number at the exit plane is unity, and the mass flow rate is the maximum (or choked) flow rate. Because the velocity of the flow is sonic at the throat for the maximum flow rate, a back pressure lower than the critical pressure cannot be sensed in the nozzle upstream flow and does not affect the flow rate.

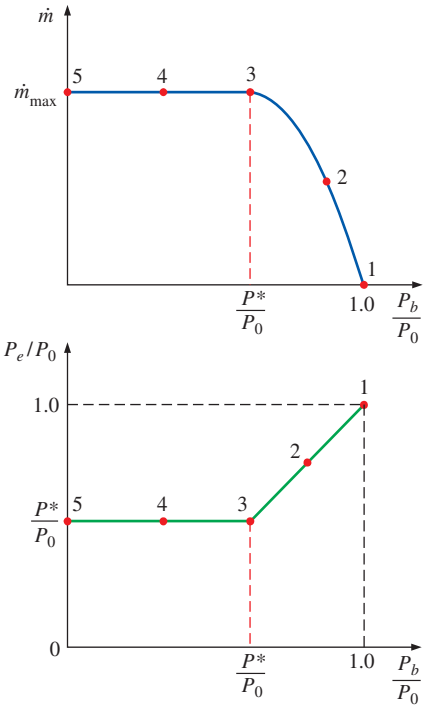

FIGURE 12–15
The effect of back pressure P_b on the mass flow rate $\dot{m}$ and the exit pressure P_e of a converging nozzle.

The effects of the stagnation temperature T_0 and stagnation pressure P_0 on the mass flow rate through a converging nozzle are illustrated in Fig. 12–16 where the mass flow rate is plotted against the static-to-stagnation pressure ratio at the throat P_t/P_0. An increase in P_0 (or a decrease of T_0) will increase the mass flow rate through the converging nozzle; a decrease in P_0 (or an increase in T_0) will decrease it. We could also conclude this by carefully observing Eqs. 12–24 and 12–25.

A relation for the variation of flow area A through the nozzle relative to throat area A^* can be obtained by combining Eqs. 12–24 and 12–25 for the same mass flow rate and stagnation properties of a particular fluid. This yields

$$\frac{A}{A^*} = \frac{1}{\text{Ma}}\left[\left(\frac{2}{k+1}\right)\left(1 + \frac{k-1}{2}\text{Ma}^2\right)\right]^{(k+1)/[2(k-1)]} \qquad \textbf{(12–26)}$$

Table A–13 gives values of A/A^* as a function of the Mach number for air ($k = 1.4$). There is one value of A/A^* for each value of the Mach number, but there are two possible values of the Mach number for each value of A/A^*—one for subsonic flow and another for supersonic flow.

Another parameter sometimes used in the analysis of one-dimensional isentropic flow of ideal gases is Ma*, which is the ratio of the local velocity to the speed of sound at the throat:

$$\text{Ma}^* = \frac{V}{c^*} \qquad \textbf{(12–27)}$$

Equation 12–27 can also be expressed as

$$\text{Ma}^* = \frac{V}{c}\frac{c}{c^*} = \frac{\text{Ma}\,c}{c^*} = \frac{\text{Ma}\sqrt{kRT}}{\sqrt{kRT^*}} = \text{Ma}\sqrt{\frac{T}{T^*}}$$

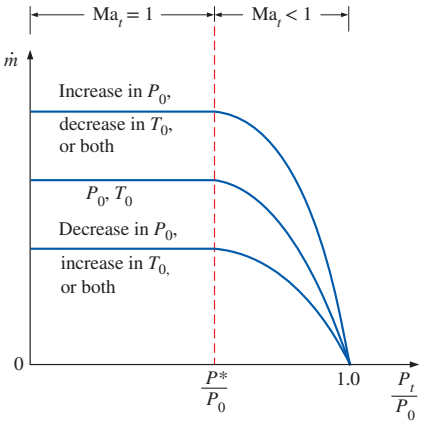

FIGURE 12–16
The variation of the mass flow rate through a nozzle with inlet stagnation properties.

Ma	Ma*	$\frac{A}{A^*}$	$\frac{P}{P_0}$	$\frac{\rho}{\rho_0}$	$\frac{T}{T_0}$
⋮	⋮	⋮	⋮	⋮	⋮
0.90	0.9146	1.0089	0.5913	⋮	⋮
1.00	1.0000	1.0000	0.5283	⋮	⋮
1.10	1.0812	1.0079	0.4684	⋮	⋮
⋮	⋮	⋮	⋮	⋮	⋮

FIGURE 12–17
Various property ratios for isentropic flow through nozzles and diffusers are listed in Table A–13 for $k = 1.4$ (air) for convenience.

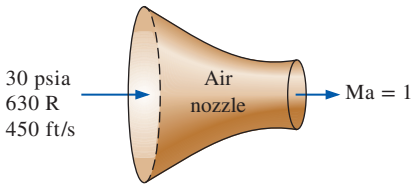

FIGURE 12–18
Schematic for Example 12–4.

where Ma is the local Mach number, T is the local temperature, and T^* is the critical temperature. Solving for T from Eq. 12–18 and for T^* from Eq. 12–21 and substituting, we get

$$\text{Ma}^* = \text{Ma}\sqrt{\frac{k+1}{2+(k-1)\text{Ma}^2}} \tag{12–28}$$

Values of Ma* are also listed in Table A–13 versus the Mach number for $k = 1.4$ (Fig. 12–17). Note that the parameter Ma* differs from the Mach number Ma in that Ma* is the local velocity nondimensionalized with respect to the sonic velocity at the *throat,* whereas Ma is the local velocity nondimensionalized with respect to the *local* sonic velocity. (Recall that the sonic velocity in a nozzle varies with temperature and thus with location.)

EXAMPLE 12–4 Isentropic Flow of Air in a Nozzle

Air enters a nozzle at 30 psia, 630 R, and a velocity of 450 ft/s (Fig. 12–18). Approximating the flow as isentropic, determine the pressure and temperature of air at a location where the air velocity equals the speed of sound. What is the ratio of the area at this location to the entrance area?

SOLUTION Air enters a nozzle at specified temperature, pressure, and velocity. The exit pressure, exit temperature, and exit-to-inlet area ratio are to be determined for a Mach number of Ma = 1 at the exit.

Assumptions **1** Air is an ideal gas with constant specific heats at room temperature. **2** Flow through the nozzle is approximated as steady, one-dimensional, and isentropic.

Properties The properties of air are $k = 1.4$ and $c_p = 0.240$ Btu/lbm·R (Table A–1E).

Analysis The properties of the fluid at the location where Ma = 1 are the critical properties, denoted by superscript *. We first determine the stagnation temperature and pressure, which remain constant throughout the nozzle since the flow is isentropic.

$$T_0 = T + \frac{V_i^2}{2c_p} = 630\text{ R} + \frac{(450\text{ ft/s})^2}{2(0.240\text{ Btu/lbm·R})}\left(\frac{1\text{ Btu/lbm}}{25{,}037\text{ ft}^2/\text{s}^2}\right) = 646.9\text{ R}$$

$$P_0 = P_i\left(\frac{T_0}{T_i}\right)^{k/(k-1)} = (30\text{ psia})\left(\frac{646.9\text{ K}}{630\text{ K}}\right)^{1.4/(1.4-1)} = 32.9\text{ psia}$$

From Table A–13 (or from Eqs. 12–18 and 12–19) at Ma = 1, we read

$T/T_0 = 0.8333$
$P/P_0 = 0.5283$

Thus,

$T = 0.8333T_0 = 0.8333(646.9\text{ R}) = \mathbf{539\text{ R}}$
$P = 0.5283P_0 = 0.5283(32.9\text{ psia}) = \mathbf{17.4\text{ psia}}$

Also,

$$c_i = \sqrt{kRT_i} = \sqrt{(1.4)(0.06855\text{ Btu/lbm·R})(630\text{ R})\left(\frac{25{,}037\text{ ft}^2/\text{s}^2}{1\text{ Btu/lbm}}\right)}$$

$$= 1230\text{ ft/s}$$

$$\text{Ma}_i = \frac{V_i}{c_i} = \frac{450\text{ ft/s}}{1230\text{ ft/s}} = 0.3657$$

From Table A–13 at this Mach number we read $A_i/A^* = 1.7426$. Thus the ratio of the throat area to the nozzle inlet area is

$$\frac{A^*}{A_i} = \frac{1}{1.7426} = \mathbf{0.574}$$

Discussion If we solve this problem using the relations for compressible isentropic flow, the results would be identical to at least three significant digits.

EXAMPLE 12–5 Air Loss from a Flat Tire

Air in an automobile tire is maintained at a pressure of 220 kPa (gage) in an environment where the atmospheric pressure is 94 kPa. The air in the tire is at the ambient temperature of 25°C. A 4-mm-diameter leak develops in the tire as a result of an accident (Fig. 12–19). Approximating the flow as isentropic determine the initial mass flow rate of air through the leak.

FIGURE 12–19
Schematic for Example 12–5.

SOLUTION A leak develops in an automobile tire as a result of an accident. The initial mass flow rate of air through the leak is to be determined.

Assumptions **1** Air is an ideal gas with constant specific heats. **2** Flow of air through the hole is isentropic.

Properties The specific gas constant of air is $R = 0.287$ kPa·m³/kg·K. The specific heat ratio of air at room temperature is $k = 1.4$.

Analysis The absolute pressure in the tire is

$$P = P_{\text{gage}} + P_{\text{atm}} = 220 + 94 = 314 \text{ kPa}$$

The critical pressure is (from Table 12–2)

$$P^* = 0.5283P_o = (0.5283)(314 \text{ kPa}) = 166 \text{ kPa} > 94 \text{ kPa}$$

Therefore, the flow is choked, and the velocity at the exit of the hole is the sonic speed. Then the flow properties at the exit become

$$\rho_0 = \frac{P_0}{RT_0} = \frac{314 \text{ kPa}}{(0.287 \text{ kPa·m}^3/\text{kg·K})(298 \text{ K})} = 3.671 \text{ kg/m}^3$$

$$\rho^* = \rho\left(\frac{2}{k+1}\right)^{1/(k-1)} = (3.671 \text{ kg/m}^3)\left(\frac{2}{1.4+1}\right)^{1/(1.4-1)} = 2.327 \text{ kg/m}^3$$

$$T^* = \frac{2}{k+1}T_0 = \frac{2}{1.4+1}(298 \text{ K}) = 248.3 \text{ K}$$

$$V = c = \sqrt{kRT^*} = \sqrt{(1.4)(0.287 \text{ kJ/kg·K})\left(\frac{1000 \text{ m}^2/\text{s}^2}{1 \text{ kJ/kg}}\right)(248.3 \text{ K})}$$

$$= 315.9 \text{ m/s}$$

Then the initial mass flow rate through the hole is

$$\dot{m} = \rho AV = (2.327 \text{ kg/m}^3)[\pi(0.004 \text{ m})^2/4](315.9 \text{ m/s}) = 0.00924 \text{ kg/s}$$

$$= \mathbf{0.554 \text{ kg/min}}$$

Discussion The mass flow rate decreases with time as the pressure inside the tire drops.

Converging–Diverging Nozzles

When we think of nozzles, we ordinarily think of flow passages whose cross-sectional area decreases in the flow direction. However, the highest velocity to which a fluid can be accelerated in a converging nozzle is limited to the sonic velocity (Ma = 1), which occurs at the exit plane (throat) of the nozzle. Accelerating a fluid to supersonic velocities (Ma > 1) can be accomplished only by attaching a diverging flow section to the subsonic nozzle at the throat. The resulting combined flow section is a converging–diverging nozzle, which is standard equipment in supersonic aircraft and rocket propulsion (Fig. 12–20).

Forcing a fluid through a converging–diverging nozzle is no guarantee that the fluid will be accelerated to a supersonic velocity. In fact, the fluid may find itself decelerating in the diverging section instead of accelerating if the back pressure is not in the right range. The state of the nozzle flow is determined by the overall pressure ratio P_b/P_0. Therefore, for given inlet conditions, the flow through a converging–diverging nozzle is governed by the back pressure P_b, as will be explained.

Consider the converging–diverging nozzle shown in Fig. 12–21. A fluid enters the nozzle with a low velocity at stagnation pressure P_0. When $P_b = P_0$ (case *A*), there is no flow through the nozzle. This is expected since the flow in a nozzle is driven by the pressure difference between the nozzle inlet and the exit. Now let us examine what happens as the back pressure is lowered.

1. When $P_0 > P_b > P_C$, the flow remains subsonic throughout the nozzle, and the mass flow is less than that for choked flow. The fluid velocity increases in the first (converging) section and reaches a maximum at the throat (but Ma < 1). However, most of the gain in velocity is lost in the second (diverging) section of the nozzle, which acts as a diffuser. The pressure

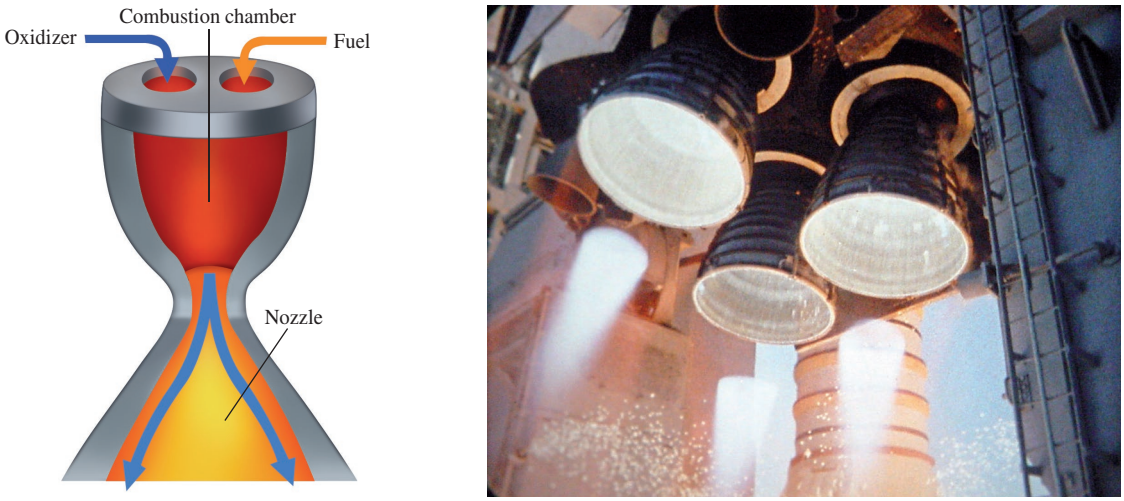

FIGURE 12–20
Converging–diverging nozzles are commonly used in rocket engines to provide high thrust.
(Right) Courtesy NASA

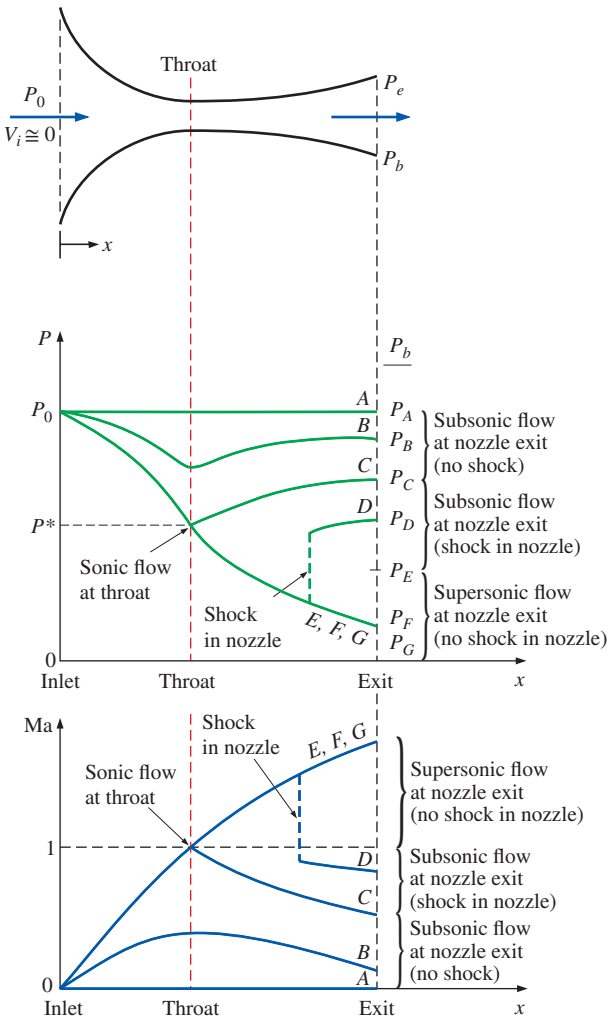

FIGURE 12–21
The effects of back pressure on the flow through a converging–diverging nozzle.

decreases in the converging section, reaches a minimum at the throat, and increases at the expense of velocity in the diverging section.

2. When $P_b = P_C$, the throat pressure becomes P^* and the fluid achieves sonic velocity at the throat. But the diverging section of the nozzle still acts as a diffuser, slowing the fluid to subsonic velocities. The mass flow rate that was increasing with decreasing P_b also reaches its maximum value. Recall that P^* is the lowest pressure that can be obtained at the throat, and the sonic velocity is the highest velocity that can be achieved with a converging nozzle. Thus, lowering P_b further has no influence on the fluid flow in the converging part of the nozzle or the mass flow rate through the nozzle. However, it does influence the character of the flow in the diverging section.
3. When $P_C > P_b > P_E$, the fluid that achieved a sonic velocity at the throat continues accelerating to supersonic velocities in the diverging section as the pressure decreases. This acceleration comes to a sudden stop, however, as a **normal shock** develops at a section between the throat and the exit

plane, which causes a sudden drop in velocity to subsonic levels and a sudden increase in pressure. The fluid then continues to decelerate further in the remaining part of the converging–diverging nozzle. Flow through the shock is highly irreversible, and thus it cannot be approximated as isentropic. The normal shock moves downstream away from the throat as P_b is decreased, and it approaches the nozzle exit plane as P_b approaches P_E.

When $P_b = P_E$, the normal shock forms at the exit plane of the nozzle. The flow is supersonic through the entire diverging section in this case, and it can be approximated as isentropic. However, the fluid velocity drops to subsonic levels just before leaving the nozzle as it crosses the normal shock. Normal shock waves are discussed in Section 12–4.

4. When $P_E > P_b > 0$, the flow in the diverging section is supersonic, and the fluid expands to P_F at the nozzle exit with no normal shock forming within the nozzle. Thus, the flow through the nozzle can be approximated as isentropic. When $P_b = P_F$, no shocks occur within or outside the nozzle. When $P_b < P_F$, irreversible mixing and expansion waves occur downstream of the exit plane of the nozzle. When $P_b > P_F$, however, the pressure of the fluid increases from P_F to P_b irreversibly in the wake of the nozzle exit, creating what are called *oblique shocks*.

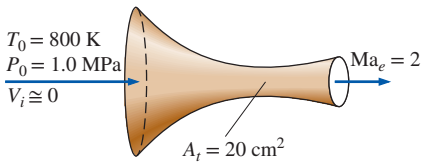

FIGURE 12–22
Schematic for Example 12–6.

EXAMPLE 12–6 **Airflow through a Converging–Diverging Nozzle**

Air enters a converging–diverging nozzle, shown in Fig. 12–22, at 1.0 MPa and 800 K with negligible velocity. The flow is steady, one-dimensional, and isentropic with $k = 1.4$. For an exit Mach number of Ma = 2 and a throat area of 20 cm^2, determine (*a*) the throat conditions, (*b*) the exit plane conditions, including the exit area, and (*c*) the mass flow rate through the nozzle.

SOLUTION Air flows through a converging–diverging nozzle. The throat and the exit conditions and the mass flow rate are to be determined.

Assumptions **1** Air is an ideal gas with constant specific heats at room temperature. **2** Flow through the nozzle is steady, one-dimensional, and isentropic.

Properties The specific heat ratio of air is given to be $k = 1.4$. The gas constant of air is 0.287 kJ/kg·K.

Analysis The exit Mach number is given to be 2. Therefore, the flow must be sonic at the throat and supersonic in the diverging section of the nozzle. Since the inlet velocity is negligible, the stagnation pressure and stagnation temperature are the same as the inlet temperature and pressure, $P_0 = 1.0$ MPa and $T_0 = 800$ K. Assuming ideal-gas behavior, the stagnation density is

$$\rho_0 = \frac{P_0}{RT_0} = \frac{1000 \text{ kPa}}{(0.287 \text{ kPa·m}^3/\text{kg·K})(800 \text{ K})} = 4.355 \text{ kg/m}^3$$

(*a*) At the throat of the nozzle Ma = 1, and from Table A–13 we read

$$\frac{P^*}{P_0} = 0.5283 \qquad \frac{T^*}{T_0} = 0.8333 \qquad \frac{\rho^*}{\rho_0} = 0.6339$$

Thus,

$$P^* = 0.5283P_0 = (0.5283)(1.0 \text{ MPa}) = \mathbf{0.5283 \text{ MPa}}$$

$$T^* = 0.8333T_0 = (0.8333)(800\ \text{K}) = \mathbf{666.6\ K}$$

$$\rho^* = 0.6339\rho_0 = (0.6339)(4.355\ \text{kg/m}^3) = \mathbf{2.761\ kg/m^3}$$

Also,

$$V^* = c^* = \sqrt{kRT^*} = \sqrt{(1.4)(0.287\ \text{kJ/kg·K})(666.6\ \text{K})\left(\frac{1000\ \text{m}^2/\text{s}^2}{1\ \text{kJ/kg}}\right)}$$

$$= \mathbf{517.5\ m/s}$$

(*b*) Since the flow is isentropic, the properties at the exit plane can also be calculated by using data from Table A–13. For Ma = 2 we read

$$\frac{P_e}{P_0} = 0.1278 \quad \frac{T_e}{T_0} = 0.5556 \quad \frac{\rho_e}{\rho_0} = 0.2300 \quad \text{Ma}_e^* = 1.6330 \quad \frac{A_e}{A^*} = 1.6875$$

Thus,

$$P_e = 0.1278P_0 = (0.1278)(1.0\ \text{MPa}) = \mathbf{0.1278\ MPa}$$

$$T_e = 0.5556T_0 = (0.5556)(800\ \text{K}) = \mathbf{444.5\ K}$$

$$\rho_e = 0.2300\rho_0 = (0.2300)(4.355\ \text{kg/m}^3) = \mathbf{1.002\ kg/m^3}$$

$$A_e = 1.6875A^* = (1.6875)(20\ \text{cm}^2) = \mathbf{33.75\ cm^2}$$

and

$$V_e = \text{Ma}_e^* c^* = (1.6330)(517.5\ \text{m/s}) = \mathbf{845.1\ m/s}$$

The nozzle exit velocity could also be determined from $V_e = \text{Ma}_e c_e$, where c_e is the speed of sound at the exit conditions:

$$V_e = \text{Ma}_e c_e = \text{Ma}_e\sqrt{kRT_e} = 2\sqrt{(1.4)(0.287\ \text{kJ/kg·K})(444.5\ \text{K})\left(\frac{1000\ \text{m}^2/\text{s}^2}{1\ \text{kJ/kg}}\right)}$$

$$= 845.2\ \text{m/s}$$

(*c*) Since the flow is steady, the mass flow rate of the fluid is the same at all sections of the nozzle. Thus it may be calculated by using properties at any cross section of the nozzle. Using the properties at the throat, we find that the mass flow rate is

$$\dot{m} = \rho^* A^* V^* = (2.761\ \text{kg/m}^3)(20 \times 10^{-4}\ \text{m}^2)(517.5\ \text{m/s}) = \mathbf{2.86\ kg/s}$$

Discussion Note that this is the highest possible mass flow rate that can flow through this nozzle for the specified inlet conditions.

12–4 ▪ SHOCK WAVES AND EXPANSION WAVES

We discussed in Chap. 2 that sound waves are caused by infinitesimally small pressure disturbances, and they travel through a medium at the speed of sound. We have also seen in the present chapter that for some back pressure values, abrupt changes in fluid properties occur in a very thin section of a converging–diverging nozzle under supersonic flow conditions,

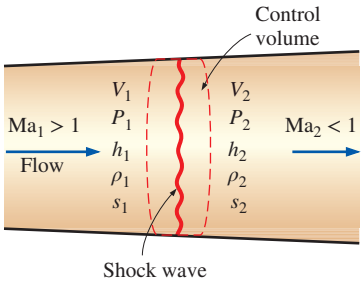

FIGURE 12–23
Control volume for flow across a normal shock wave.

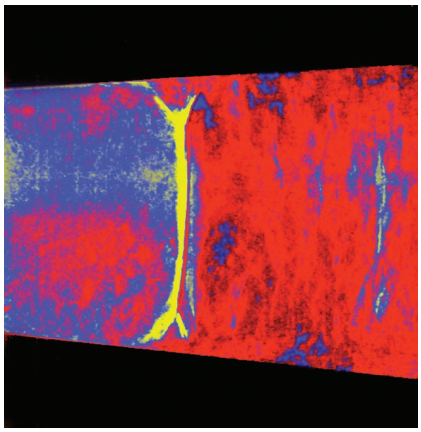

FIGURE 12–24
Schlieren image of a normal shock in a Laval nozzle. The Mach number in the nozzle just upstream (to the left) of the shock wave is about 1.3. Boundary layers distort the shape of the normal shock near the walls and lead to flow separation beneath the shock.

creating a **shock wave**. It is of interest to study the conditions under which shock waves develop and how they affect the flow.

Normal Shocks

First we consider shock waves that occur in a plane normal to the direction of flow, called **normal shock waves**. The flow process through the shock wave is highly irreversible and *cannot* be approximated as being isentropic.

Next we follow the footsteps of Pierre Laplace (1749–1827), G. F. Bernhard Riemann (1826–1866), William Rankine (1820–1872), Pierre Henry Hugoniot (1851–1887), Lord Rayleigh (1842–1919), and G. I. Taylor (1886–1975) and develop relationships for the flow properties before and after the shock. We do this by applying the conservation of mass, momentum, and energy relations as well as some property relations to a stationary control volume that contains the shock, as shown in Fig. 12–23. The normal shock waves are extremely thin, so the entrance and exit flow areas for the control volume are approximately equal (Fig. 12–24).

We assume steady flow with no heat and work interactions and no potential energy changes. Denoting the properties upstream of the shock by the subscript 1 and those downstream of the shock by 2, we have the following:

Conservation of mass:
$$\rho_1 A V_1 = \rho_2 A V_2 \tag{12–29}$$

or

$$\rho_1 V_1 = \rho_2 V_2$$

Conservation of energy:
$$h_1 + \frac{V_1^2}{2} = h_2 + \frac{V_2^2}{2} \tag{12–30}$$

or

$$h_{01} = h_{02} \tag{12–31}$$

Linear momentum equation: Rearranging Eq. 12–14 and integrating yield

$$A(P_1 - P_2) = \dot{m}(V_2 - V_1) \tag{12–32}$$

Increase of entropy:
$$s_2 - s_1 \geq 0 \tag{12–33}$$

We can combine the conservation of mass and energy relations into a single equation and plot it on an *h-s* diagram, using property relations. The resultant curve is called the **Fanno line**, and it is the locus of states that have the same value of stagnation enthalpy and mass flux (mass flow per unit flow area). Likewise, combining the conservation of mass and momentum equations into a single equation and plotting it on the *h-s* diagram yield a curve called the **Rayleigh line**. Both these lines are shown on the *h-s* diagram in Fig. 12–25. As proved later in Example 12–7, the points of maximum entropy on these lines (points *a* and *b*) correspond to Ma = 1. The state on the upper part of each curve is subsonic and on the lower part supersonic.

The Fanno and Rayleigh lines intersect at two points (points 1 and 2), which represent the two states at which all three conservation equations are satisfied. One of these (state 1) corresponds to the state before the shock,

and the other (state 2) corresponds to the state after the shock. Note that the flow is supersonic before the shock and subsonic afterward. Therefore the flow must change from supersonic to subsonic if a shock is to occur. The larger the Mach number before the shock, the stronger the shock will be. In the limiting case of Ma = 1, the shock wave simply becomes a sound wave. Notice from Fig. 12–25 that entropy increases, $s_2 > s_1$. This is expected since the flow through the shock is adiabatic but irreversible.

The conservation of energy principle (Eq. 12–31) requires that the stagnation enthalpy remain constant across the shock; $h_{01} = h_{02}$. For ideal gases $h = h(T)$, and thus

$$T_{01} = T_{02} \tag{12–34}$$

That is, the stagnation temperature of an ideal gas also remains constant across the shock. Note, however, that the stagnation pressure decreases across the shock because of the irreversibilities, while the ordinary (static) temperature rises drastically because of the conversion of kinetic energy into enthalpy due to a large drop in fluid velocity (see Fig. 12–26).

We now develop relations between various properties before and after the shock for an ideal gas with constant specific heats. A relation for the ratio of the static temperatures T_2/T_1 is obtained by applying Eq. 12–18 twice:

$$\frac{T_{01}}{T_1} = 1 + \left(\frac{k-1}{2}\right)\text{Ma}_1^2 \quad \text{and} \quad \frac{T_{02}}{T_2} = 1 + \left(\frac{k-1}{2}\right)\text{Ma}_2^2$$

Dividing the first equation by the second one and noting that $T_{01} = T_{02}$, we have

$$\frac{T_2}{T_1} = \frac{1 + \text{Ma}_1^2(k-1)/2}{1 + \text{Ma}_2^2(k-1)/2} \tag{12–35}$$

From the ideal-gas equation of state,

$$\rho_1 = \frac{P_1}{RT_1} \quad \text{and} \quad \rho_2 = \frac{P_2}{RT_2}$$

Substituting these into the conservation of mass relation $\rho_1 V_1 = \rho_2 V_2$ and noting that $\text{Ma} = V/c$ and $c = \sqrt{kRT}$, we have

$$\frac{T_2}{T_1} = \frac{P_2 V_2}{P_1 V_1} = \frac{P_2 \text{Ma}_2 c_2}{P_1 \text{Ma}_1 c_1} = \frac{P_2 \text{Ma}_2 \sqrt{T_2}}{P_1 \text{Ma}_1 \sqrt{T_1}} = \left(\frac{P_2}{P_1}\right)^2 \left(\frac{\text{Ma}_2}{\text{Ma}_1}\right)^2 \tag{12–36}$$

Combining Eqs. 12–35 and 12–36 gives the pressure ratio across the shock:

Fanno line:

$$\frac{P_2}{P_1} = \frac{\text{Ma}_1\sqrt{1 + \text{Ma}_1^2(k-1)/2}}{\text{Ma}_2\sqrt{1 + \text{Ma}_2^2(k-1)/2}} \tag{12–37}$$

Equation 12–37 is a combination of the conservation of mass and energy equations; thus, it is also the equation of the Fanno line for an ideal gas with constant specific heats. A similar relation for the Rayleigh line is obtained by combining the conservation of mass and momentum equations. From Eq. 12–32,

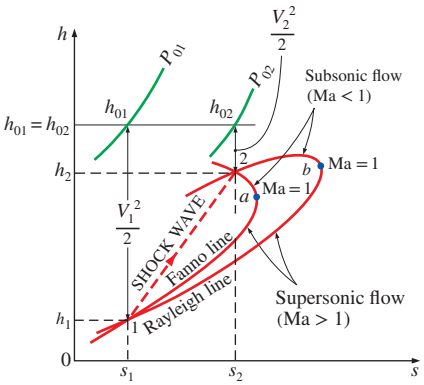

FIGURE 12–25
The *h*-*s* diagram for flow across a normal shock.

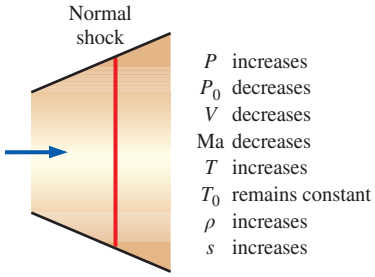

FIGURE 12–26
Variation of flow properties across a normal shock in an ideal gas.

FIGURE 12–27
The air inlet of a supersonic fighter jet is designed such that a shock wave at the inlet decelerates the air to subsonic velocities, increasing the pressure and temperature of the air before it enters the engine.

$$P_1 - P_2 = \frac{\dot{m}}{A}(V_2 - V_1) = \rho_2 V_2^2 - \rho_1 V_1^2$$

However,

$$\rho V^2 = \left(\frac{P}{RT}\right)(\text{Ma}\, c)^2 = \left(\frac{P}{RT}\right)(\text{Ma}\sqrt{kRT})^2 = Pk\,\text{Ma}^2$$

Thus,

$$P_1(1 + k\text{Ma}_1^2) = P_2(1 + k\text{Ma}_2^2)$$

or

Rayleigh line:
$$\frac{P_2}{P_1} = \frac{1 + k\text{Ma}_1^2}{1 + k\text{Ma}_2^2} \qquad \textbf{(12–38)}$$

Combining Eqs. 12–37 and 12–38 yields

$$\text{Ma}_2^2 = \frac{\text{Ma}_1^2 + 2/(k-1)}{2\text{Ma}_1^2\, k/(k-1) - 1} \qquad \textbf{(12–39)}$$

This represents the intersections of the Fanno and Rayleigh lines and relates the Mach number upstream of the shock to that downstream of the shock.

The occurrence of shock waves is not limited to supersonic nozzles only. This phenomenon is also observed at the engine inlet of supersonic aircraft, where the air passes through a shock and decelerates to subsonic velocities before entering the diffuser of the engine (Fig. 12–27). Explosions also produce powerful expanding spherical normal shocks, which can be very destructive (Fig. 12–28).

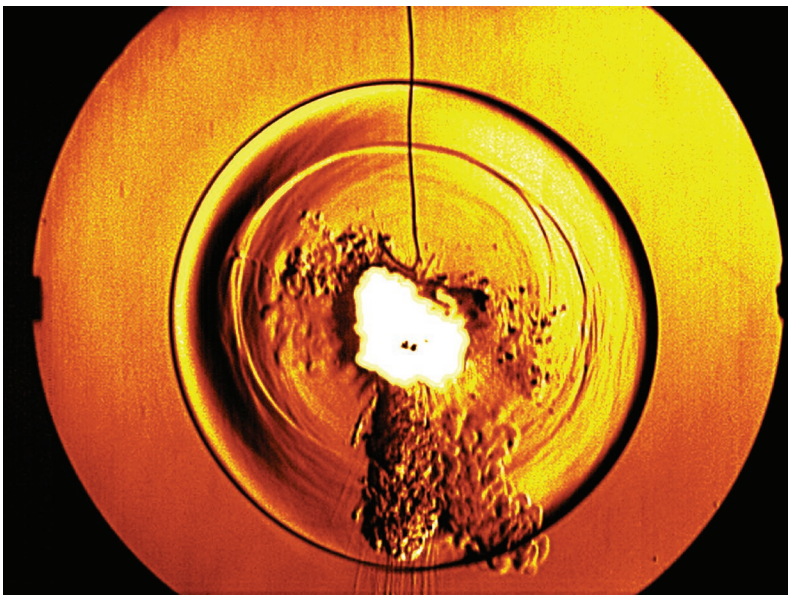

FIGURE 12–28
Schlieren image of the blast wave (expanding spherical normal shock) produced by the explosion of a firecracker. The shock expanded radially outward in all directions at a supersonic speed that decreased with radius from the center of the explosion. A microphone sensed the sudden change in pressure of the passing shock wave and triggered the microsecond flashlamp that exposed the photograph.

Various flow property ratios across the shock are listed in Table A–14 for an ideal gas with $k = 1.4$. Inspection of this table reveals that Ma_2 (the Mach number after the shock) is always less than 1 and that the larger the supersonic Mach number before the shock, the smaller the subsonic Mach number after the shock. Also, we see that the static pressure, temperature, and density all increase after the shock while the stagnation pressure decreases.

The entropy change across the shock is obtained by applying the entropy-change equation for an ideal gas across the shock:

$$s_2 - s_1 = c_P \ln \frac{T_2}{T_1} - R \ln \frac{P_2}{P_1} \qquad \textbf{(12–40)}$$

which can be expressed in terms of k, R, and Ma_1 by using the relations developed earlier in this section. A plot of nondimensional entropy change across the normal shock $(s_2 - s_1)/R$ versus Ma_1 is shown in Fig. 12–29. Since the flow across the shock is adiabatic and irreversible, the second law of thermodynamics requires that the entropy increase across the shock wave. Thus, a shock wave cannot exist for values of Ma_1 less than unity where the entropy change would be negative. For adiabatic flows, shock waves can exist only for supersonic flows, $\text{Ma}_1 > 1$.

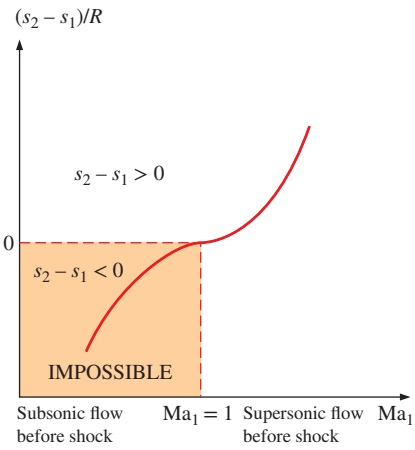

FIGURE 12–29
Entropy change across a normal shock.

EXAMPLE 12–7 The Point of Maximum Entropy on the Fanno Line

Show that the point of maximum entropy on the Fanno line (point a of Fig. 12–25) for the adiabatic steady flow of a fluid in a duct corresponds to the sonic velocity, $\text{Ma} = 1$.

SOLUTION It is to be shown that the point of maximum entropy on the Fanno line for steady adiabatic flow corresponds to sonic velocity.

Assumption The flow is steady, adiabatic, and one-dimensional.

Analysis In the absence of any heat and work interactions and potential energy changes, the steady-flow energy equation reduces to

$$h + \frac{V^2}{2} = \text{constant}$$

Differentiating yields

$$dh + V\,dV = 0$$

For a very thin shock with negligible change of duct area across the shock, the steady-flow continuity (conservation of mass) equation is expressed as

$$\rho V = \text{constant}$$

Differentiating, we have

$$\rho\,dV + V\,d\rho = 0$$

Solving for dV gives

$$dV = -V\frac{d\rho}{\rho}$$

Combining this with the energy equation, we have

$$dh - V^2 \frac{d\rho}{\rho} = 0$$

which is the equation for the Fanno line in differential form. At point a (the point of maximum entropy) $ds = 0$. Then from the second $T\,ds$ relation ($T\,ds = dh - \upsilon\,dP$) we have $dh = \upsilon\,dP = dP/\rho$. Substituting yields

$$\frac{dP}{\rho} - V^2 \frac{d\rho}{\rho} = 0 \qquad \text{at } s = \text{constant}$$

Solving for V, we have

$$V = \left(\frac{\partial P}{\partial \rho}\right)_s^{1/2}$$

which is the relation for the speed of sound, Eq. 12–9. Thus $V = c$ and the proof is complete.

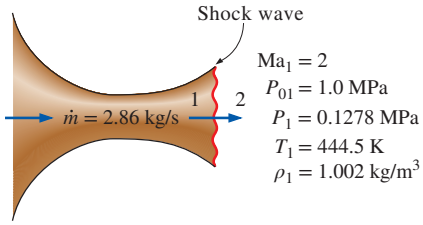

FIGURE 12–30
Schematic for Example 12–8.

EXAMPLE 12–8 Shock Wave in a Converging–Diverging Nozzle

If the air flowing through the converging–diverging nozzle of Example 12–6 experiences a normal shock wave at the nozzle exit plane (Fig. 12–30), determine the following after the shock: (*a*) the stagnation pressure, static pressure, static temperature, and static density; (*b*) the entropy change across the shock; (*c*) the exit velocity; and (*d*) the mass flow rate through the nozzle. Approximate the flow as steady, one-dimensional, and isentropic with $k = 1.4$ from the nozzle inlet to the shock location.

SOLUTION Air flowing through a converging–diverging nozzle experiences a normal shock at the exit. The effect of the shock wave on various properties is to be determined.

Assumptions **1** Air is an ideal gas with constant specific heats at room temperature. **2** Flow through the nozzle is steady, one-dimensional, and isentropic before the shock occurs. **3** The shock wave occurs at the exit plane.

Properties The constant-pressure specific heat and the specific heat ratio of air are $c_p = 1.005$ kJ/kg·K and $k = 1.4$. The gas constant of air is 0.287 kJ/kg·K.

Analysis (*a*) The fluid properties at the exit of the nozzle just before the shock (denoted by subscript 1) are those evaluated in Example 12–6 at the nozzle exit to be

$$P_{01} = 1.0 \text{ MPa} \quad P_1 = 0.1278 \text{ MPa} \quad T_1 = 444.5 \text{ K} \quad \rho_1 = 1.002 \text{ kg/m}^3$$

The fluid properties after the shock (denoted by subscript 2) are related to those before the shock through the functions listed in Table A–14. For $Ma_1 = 2.0$, we read

$$Ma_2 = 0.5774 \quad \frac{P_{02}}{P_{01}} = 0.7209 \quad \frac{P_2}{P_1} = 4.5000 \quad \frac{T_2}{T_1} = 1.6875 \quad \frac{\rho_2}{\rho_1} = 2.6667$$

Then the stagnation pressure P_{02}, static pressure P_2, static temperature T_2, and static density ρ_2 after the shock are

$$P_{02} = 0.7209P_{01} = (0.7209)(1.0 \text{ MPa}) = \mathbf{0.721 \text{ MPa}}$$

$$P_2 = 4.5000P_1 = (4.5000)(0.1278 \text{ MPa}) = \mathbf{0.575 \text{ MPa}}$$

$$T_2 = 1.6875T_1 = (1.6875)(444.5 \text{ K}) = \mathbf{750 \text{ K}}$$

$$\rho_2 = 2.6667\rho_1 = (2.6667)(1.002 \text{ kg/m}^3) = \mathbf{2.67 \text{ kg/m}^3}$$

(*b*) The entropy change across the shock is

$$s_2 - s_1 = c_\rho \ln \frac{T_2}{T_1} - R \ln \frac{P_2}{P_1}$$

$$= (1.005 \text{ kJ/kg·K}) \ln (1.6875) - (0.287 \text{ kJ/kg·K}) \ln (4.5000)$$

$$= \mathbf{0.0942 \text{ kJ/kg·K}}$$

Thus, the entropy of the air increases as it passes through a normal shock, which is highly irreversible.

(*c*) The air velocity after the shock is determined from $V_2 = \text{Ma}_2 c_2$, where c_2 is the speed of sound at the exit conditions after the shock:

$$V_2 = \text{Ma}_2 c_2 = \text{Ma}_2 \sqrt{kRT_2}$$

$$= (0.5774)\sqrt{(1.4)(0.287 \text{ kJ/kg·K})(750.1 \text{ K})\left(\frac{1000 \text{ m}^2/\text{s}^2}{1 \text{ kJ/kg}}\right)}$$

$$= \mathbf{317 \text{ m/s}}$$

(*d*) The mass flow rate through a converging–diverging nozzle with sonic conditions at the throat is not affected by the presence of shock waves in the nozzle. Therefore, the mass flow rate in this case is the same as that determined in Example 12–6:

$$\dot{m} = \mathbf{2.86 \text{ kg/s}}$$

Discussion This result can easily be verified by using property values at the nozzle exit after the shock at all Mach numbers significantly greater than unity.

Example 12–8 illustrates that the stagnation pressure and velocity decrease while the static pressure, temperature, density, and entropy increase across the shock (Fig. 12–31). The rise in the temperature of the fluid downstream of a shock wave is of major concern to the aerospace engineer because it creates heat transfer problems on the leading edges of wings and nose cones of space reentry vehicles and the recently proposed hypersonic space planes. Overheating, in fact, led to the tragic loss of the space shuttle *Columbia* in February of 2003 as it was reentering earth's atmosphere.

FIGURE 12–31
When a lion tamer cracks his whip, a weak spherical shock wave forms near the tip and spreads out radially; the pressure inside the expanding shock wave is higher than ambient air pressure, and this is what causes the crack when the shock wave reaches the lion's ear.

Oblique Shocks

Not all shock waves are normal shocks (perpendicular to the flow direction). For example, when the space shuttle travels at supersonic speeds through the atmosphere, it produces a complicated shock pattern consisting of inclined

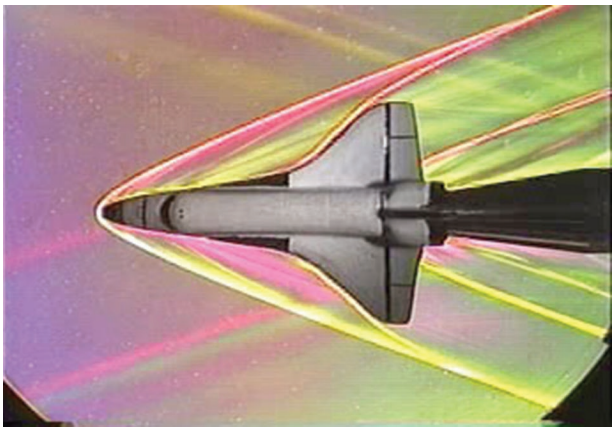

FIGURE 12–32
Schlieren image of a small model of the space shuttle orbiter being tested at Mach 3 in the supersonic wind tunnel of the Penn State Gas Dynamics Lab. Several *oblique shocks* are seen in the air surrounding the spacecraft.

shock waves called **oblique shocks** (Fig. 12–32). As you can see, some portions of an oblique shock are curved, while other portions are straight.

First, we consider straight oblique shocks, like that produced when a uniform supersonic flow ($Ma_1 > 1$) impinges on a slender, two-dimensional wedge of half-angle δ (Fig. 12–33). Since information about the wedge cannot travel upstream in a supersonic flow, the fluid "knows" nothing about the wedge until it hits the nose. At that point, since the fluid cannot flow *through* the wedge, it turns suddenly through an angle called the **turning angle** or **deflection angle** θ. The result is a straight oblique shock wave, aligned at **shock angle** or **wave angle** β, measured relative to the oncoming flow (Fig. 12–34). To conserve mass, β must obviously be greater than δ. Since the Reynolds number of supersonic flows is typically large, the boundary layer growing along the wedge is very thin, and we ignore its effects. The flow therefore turns by the same angle as the wedge; namely, deflection angle θ is equal to wedge half-angle δ. If we take into account the displacement thickness effect of the boundary layer (Chap. 10), the deflection angle θ of the oblique shock turns out to be slightly greater than wedge half-angle δ.

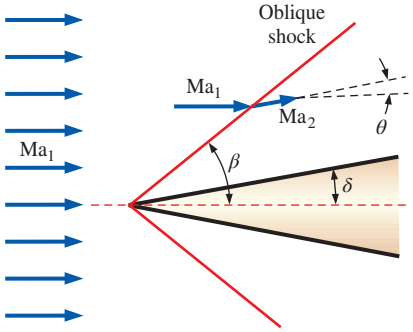

FIGURE 12–33
An oblique shock of *shock angle* β formed by a slender, two-dimensional wedge of half-angle δ. The flow is turned by *deflection angle* θ downstream of the shock, and the Mach number decreases.

Like normal shocks, the Mach number decreases across an oblique shock, and oblique shocks are possible only if the upstream flow is supersonic. However, unlike normal shocks, in which the downstream Mach number is always subsonic, Ma_2 downstream of an oblique shock can be subsonic, sonic, or supersonic, depending on the upstream Mach number Ma_1 and the turning angle.

We analyze a straight oblique shock in Fig. 12–34 by decomposing the velocity vectors upstream and downstream of the shock into normal and tangential components, and considering a small control volume around the shock. Upstream of the shock, all fluid properties (velocity, density, pressure, etc.) along the lower left face of the control volume are identical to those along the upper right face. The same is true downstream of the shock. Therefore, the mass flow rates entering and leaving those two faces cancel each other out, and conservation of mass reduces to

$$\rho_1 V_{1,n} A = \rho_2 V_{2,n} A \quad \rightarrow \quad \rho_1 V_{1,n} = \rho_2 V_{2,n} \qquad \textbf{(12–41)}$$

where A is the area of the control surface that is parallel to the shock. Since A is the same on either side of the shock, it has dropped out of Eq. 12–41.

As you might expect, the tangential component of velocity (parallel to the oblique shock) does not change across the shock, i.e., $V_{1,t} = V_{2,t}$. This is easily proven by applying the tangential momentum equation to the control volume.

When we apply conservation of momentum in the direction *normal* to the oblique shock, the only forces are pressure forces, and we get

$$P_1 A - P_2 A = \rho V_{2,n} A V_{2,n} - \rho V_{1,n} A V_{1,n} \rightarrow P_1 - P_2 = \rho_2 V_{2,n}^2 - \rho_1 V_{1,n}^2 \qquad \textbf{(12–42)}$$

Finally, since there is no work done by the control volume and no heat transfer into or out of the control volume, stagnation enthalpy does *not* change across an oblique shock, and conservation of energy yields

$$h_{01} = h_{02} = h_0 \rightarrow h_1 + \frac{1}{2} V_{1,n}^2 + \frac{1}{2} V_{1,t}^2 = h_2 + \frac{1}{2} V_{2,n}^2 + \frac{1}{2} V_{2,t}^2$$

But since $V_{1,t} = V_{2,t}$, this equation reduces to

$$h_1 + \frac{1}{2} V_{1,n}^2 = h_2 + \frac{1}{2} V_{2,n}^2 \qquad \textbf{(12–43)}$$

Careful comparison reveals that the equations for conservation of mass, momentum, and energy (Eqs. 12–41 through 12–43) across an oblique shock are identical to those across a normal shock, except that they are written in terms of the *normal* velocity component only. Therefore, the normal shock relations derived previously apply to oblique shocks as well, but must be written in terms of Mach numbers $\mathrm{Ma}_{1,n}$ and $\mathrm{Ma}_{2,n}$ normal to the oblique shock. This is most easily visualized by rotating the velocity vectors in Fig. 12–34 by angle $\pi/2 - \beta$, so that the oblique shock appears to be vertical (Fig. 12–35). Trigonometry yields

$$\mathrm{Ma}_{1,n} = \mathrm{Ma}_1 \sin\beta \quad \text{and} \quad \mathrm{Ma}_{2,n} = \mathrm{Ma}_2 \sin(\beta - \theta) \qquad \textbf{(12–44)}$$

where $\mathrm{Ma}_{1,n} = V_{1,n}/c_1$ and $\mathrm{Ma}_{2,n} = V_{2,n}/c_2$. From the point of view shown in Fig. 12–35, we see what looks like a normal shock, but with some superposed tangential flow "coming along for the ride." Thus,

> All the equations, shock tables, etc., for normal shocks apply to oblique shocks as well, provided that we use only the **normal** components of the Mach number.

In fact, you may think of normal shocks as special oblique shocks in which shock angle $\beta = \pi/2$, or 90°. We recognize immediately that an oblique shock can exist only if $\mathrm{Ma}_{1,n} > 1$ and $\mathrm{Ma}_{2,n} < 1$. The normal shock equations appropriate for oblique shocks in an ideal gas are summarized in Fig. 12–36 in terms of $\mathrm{Ma}_{1,n}$.

For known shock angle β and known upstream Mach number Ma_1, we use the first part of Eq. 12–44 to calculate $\mathrm{Ma}_{1,n}$, and then use the normal shock tables (or their corresponding equations) to obtain $\mathrm{Ma}_{2,n}$. If we also knew the deflection angle θ, we could calculate Ma_2 from the second part of Eq. 12–44. But, in a typical application, we know either β or θ, but not both. Fortunately, a bit more algebra provides us with a relationship between θ,

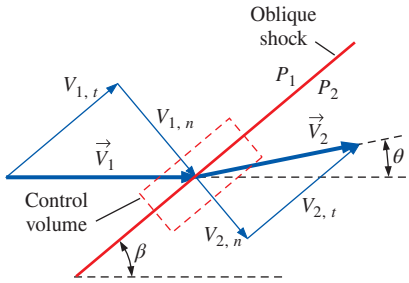

FIGURE 12–34
Velocity vectors through an oblique shock of shock angle β and deflection angle θ.

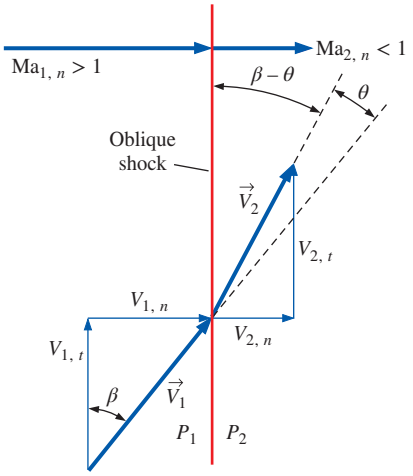

FIGURE 12–35
The same velocity vectors of Fig. 12–34, but rotated by angle $\pi/2 - \beta$, so that the oblique shock is vertical. Normal Mach numbers $\mathrm{Ma}_{1,n}$ and $\mathrm{Ma}_{2,n}$ are also defined.

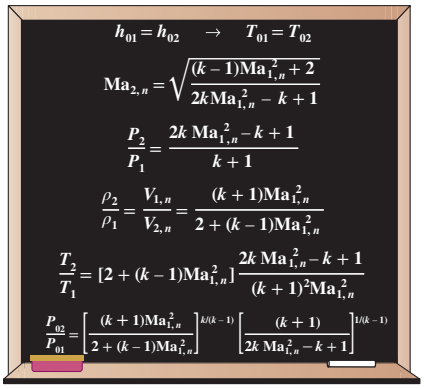

FIGURE 12–36
Relationships across an oblique shock for an ideal gas in terms of the normal component of upstream Mach number $\mathrm{Ma}_{1,n}$.

β, and Ma_1. We begin by noting that $\tan\beta = V_{1,n}/V_{1,t}$ and $\tan(\beta - \theta) = V_{2,n}/V_{2,t}$ (Fig. 12–35). But since $V_{1,t} = V_{2,t}$, we combine these two expressions to yield

$$\frac{V_{2,n}}{V_{1,n}} = \frac{\tan(\beta-\theta)}{\tan\beta} = \frac{2 + (k-1)\mathrm{Ma}_{1,n}^2}{(k+1)\mathrm{Ma}_{1,n}^2} = \frac{2 + (k-1)\mathrm{Ma}_1^2\sin^2\beta}{(k+1)\mathrm{Ma}_1^2\sin^2\beta} \qquad \textbf{(12–45)}$$

where we have also used Eq. 12–44 and the fourth equation of Fig. 12–36. We apply trigonometric identities for $\cos 2\beta$ and $\tan(\beta - \theta)$, namely,

$$\cos 2\beta = \cos^2\beta - \sin^2\beta \quad \text{and} \quad \tan(\beta-\theta) = \frac{\tan\beta - \tan\theta}{1 + \tan\beta\tan\theta}$$

After some algebra, Eq. 12–45 reduces to

The θ-β-Ma relationship:
$$\tan\theta = \frac{2\cot\beta(\mathrm{Ma}_1^2\sin^2\beta - 1)}{\mathrm{Ma}_1^2(k + \cos 2\beta) + 2} \qquad \textbf{(12–46)}$$

Equation 12–46 provides deflection angle θ as a unique function of shock angle β, specific heat ratio k, and upstream Mach number Ma_1. For air ($k = 1.4$), we plot θ versus β for several values of Ma_1 in Fig. 12–37. We note that this plot is often presented with the axes reversed (β versus θ) in compressible flow textbooks, since, physically, shock angle β is determined by deflection angle θ.

Much can be learned by studying Fig. 12–37, and we list some observations here:

- Figure 12–37 displays the full range of possible shock waves at a given free-stream Mach number, from the weakest to the strongest. For any value of Mach number Ma_1 greater than 1, the possible values of θ range from $\theta = 0°$ at some value of β between 0 and 90°, to a maximum value $\theta = \theta_{max}$ at an intermediate value of β, and then back to $\theta = 0°$ at $\beta = 90°$. Straight oblique shocks for θ or β outside of this range *cannot* and *do not* exist. At $\mathrm{Ma}_1 = 1.5$, for example, straight oblique shocks cannot exist in

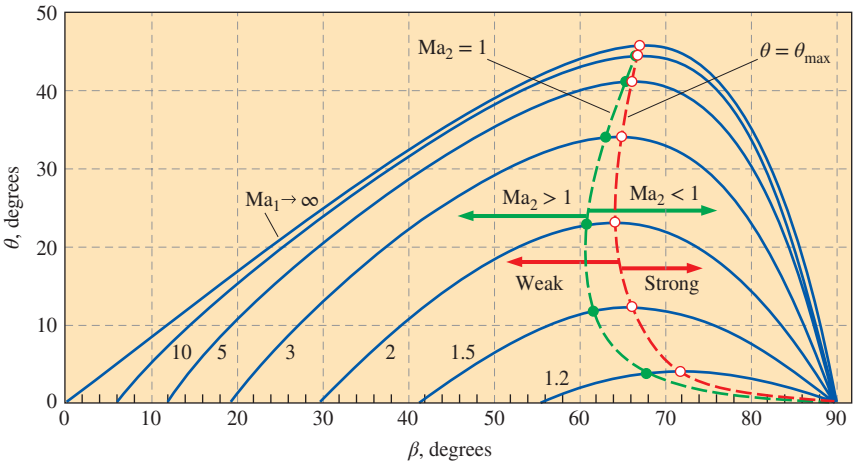

FIGURE 12–37
The dependence of straight oblique shock deflection angle θ on shock angle β for several values of upstream Mach number Ma_1. Calculations are for an ideal gas with $k = 1.4$. The dashed red line connects points of maximum deflection angle ($\theta = \theta_{max}$). *Weak oblique shocks* are to the left of this line, while *strong oblique shocks* are to the right of this line. The dashed green line connects points where the downstream Mach number is *sonic* ($\mathrm{Ma}_2 = 1$). *Supersonic downstream flow* ($\mathrm{Ma}_2 > 1$) is to the left of this line, while *subsonic downstream flow* ($\mathrm{Ma}_2 < 1$) is to the right of this line.

air with shock angle β less than about 42°, nor with deflection angle θ greater than about 12°. If the wedge half-angle is greater than θ_{max}, the shock becomes curved and detaches from the nose of the wedge, forming what is called a **detached oblique shock** or a **bow wave** (Fig. 12–38). The shock angle β of the detached shock is 90° at the nose, but β decreases as the shock curves downstream. Detached shocks are much more complicated than simple straight oblique shocks to analyze. In fact, no simple solutions exist, and prediction of detached shocks requires computational methods (Chap. 15).

- Similar oblique shock behavior is observed in *axisymmetric flow* over cones, as in Fig. 12–39, although the θ-β-Ma relationship for axisymmetric flows differs from that of Eq. 12–46.
- When supersonic flow impinges on a blunt (or bluff) body—a body *without* a sharply pointed nose, the wedge half-angle δ at the nose is 90°, and an attached oblique shock cannot exist, regardless of Mach number. In fact, a detached oblique shock occurs in front of *all* such blunt-nosed bodies, whether two-dimensional, axisymmetric, or fully three-dimensional. For example, a detached oblique shock is seen in front of the space shuttle model in Fig. 12–32 and in front of a sphere in Fig. 12–40.
- While θ is a unique function of Ma_1 and β for a given value of k, there are *two* possible values of β for $\theta < \theta_{max}$. The dashed red line in Fig. 12–37 passes through the locus of θ_{max} values, dividing the shocks into **weak oblique shocks** (the smaller value of β) and **strong oblique shocks** (the larger value of β). At a given value of θ, the weak shock is more common and is "preferred" by the flow unless the downstream pressure conditions are high enough for the formation of a strong shock.
- For a given upstream Mach number Ma_1, there is a unique value of θ for which the downstream Mach number Ma_2 is exactly 1. The dashed green line in Fig. 12–37 passes through the locus of values where $Ma_2 = 1$. To the left of this line, $Ma_2 > 1$, and to the right of this line, $Ma_2 < 1$. Downstream sonic conditions occur on the weak shock side of the plot, with θ very close to θ_{max}. Thus, the flow downstream of a strong oblique shock is *always subsonic* ($Ma_2 < 1$). The flow downstream of a weak oblique shock remains *supersonic,* except for a narrow range of θ just below θ_{max}, where it is subsonic, although it is still called a weak oblique shock.

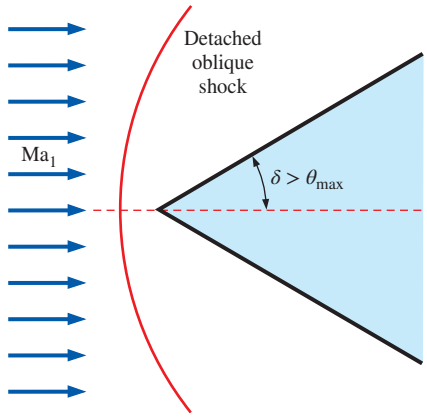

FIGURE 12–38
A *detached oblique shock* occurs upstream of a two-dimensional wedge of half-angle δ when δ is greater than the maximum possible deflection angle θ. A shock of this kind is called a *bow wave* because of its resemblance to the water wave that forms at the bow of a ship.

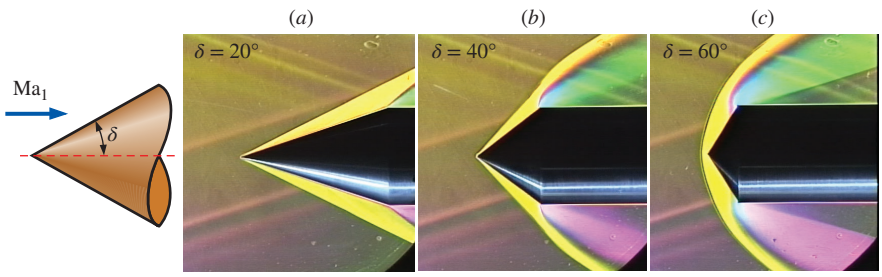

FIGURE 12–39
Still frames from schlieren videography illustrating the detachment of an oblique shock from a cone with increasing cone half-angle δ in air at Mach 3. At (*a*) $\delta = 20°$ and (*b*) $\delta = 40°$, the oblique shock remains attached, but by (*c*) $\delta = 60°$, the oblique shock has detached, forming a bow wave.

FIGURE 12–40
Color schlieren image of Mach 3.0 flow from left to right over a sphere. A curved shock wave called a bow shock forms in front of the sphere and curves downstream.

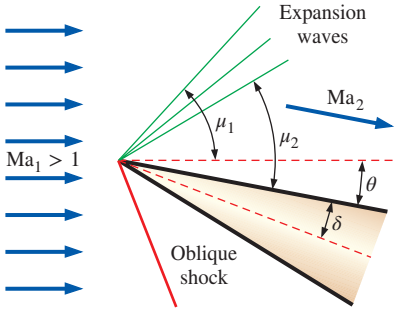

FIGURE 12–41
An expansion fan in the upper portion of the flow formed by a two-dimensional wedge at an angle of attack in a supersonic flow. The flow is turned by angle θ, and the Mach number increases across the expansion fan. Mach angles upstream and downstream of the expansion fan are indicated. Only three expansion waves are shown for simplicity, but in fact, there are an infinite number of them. (An oblique shock is also present in the bottom portion of this flow.)

- As the upstream Mach number approaches infinity, straight oblique shocks become possible for any β between 0 and 90°, but the maximum possible turning angle for $k = 1.4$ (air) is $\theta_{max} \cong 45.6°$, which occurs at $\beta = 67.8°$. Straight oblique shocks with turning angles above this value of θ_{max} are not possible, regardless of the Mach number.
- For a given value of upstream Mach number, there are two shock angles where there is *no turning of the flow* ($\theta = 0°$): the strong case, $\beta = 90°$, corresponds to a *normal shock,* and the weak case, $\beta = \beta_{min}$, represents the weakest possible oblique shock at that Mach number, which is called a **Mach wave**. Mach waves are caused, for example, by very small non-uniformities on the walls of a supersonic wind tunnel (several can be seen in Figs. 12–32 and 12–39). Mach waves have no effect on the flow, since the shock is vanishingly weak. In fact, in the limit, Mach waves are *isentropic*. The shock angle for Mach waves is a unique function of the Mach number and is given the symbol μ, not to be confused with the coefficient of viscosity. Angle μ is called the **Mach angle** and is found by setting θ equal to zero in Eq. 12–46, solving for $\beta = \mu$, and taking the smaller root. We get

Mach angle: $$\mu = \sin^{-1}(1/\text{Ma}_1) \qquad \textbf{(12–47)}$$

Since the specific heat ratio appears only in the denominator of Eq. 12–46, μ is independent of k. Thus, we can estimate the Mach number of any supersonic flow simply by measuring the Mach angle and applying Eq. 12–47.

Prandtl–Meyer Expansion Waves

We now address situations where supersonic flow is turned in the *opposite* direction, such as in the upper portion of a two-dimensional wedge at an angle of attack greater than its half-angle δ (Fig. 12–41). We refer to this type of flow as an **expanding flow**, whereas a flow that produces an oblique shock may be called a **compressing flow**. As previously, the flow changes direction to conserve mass. However, unlike a compressing flow, an expanding flow does *not* result in a shock wave. Rather, a continuous expanding region called an **expansion fan** appears, composed of an infinite number of Mach waves called **Prandtl–Meyer expansion waves**. In other words, the flow does not turn suddenly, as through a shock, but *gradually*—each successive Mach wave turns the flow by an infinitesimal amount. Since each individual expansion wave is nearly isentropic, the flow across the entire expansion fan is also nearly isentropic. The Mach number downstream of the expansion *increases* ($\text{Ma}_2 > \text{Ma}_1$), while pressure, density, and temperature *decrease,* just as they do in the supersonic (expanding) portion of a converging–diverging nozzle.

Prandtl–Meyer expansion waves are inclined at the local Mach angle μ, as sketched in Fig. 12–41. The Mach angle of the first expansion wave is easily determined as $\mu_1 = \sin^{-1}(1/\text{Ma}_1)$. Similarly, $\mu_2 = \sin^{-1}(1/\text{Ma}_2)$, where we must be careful to measure the angle relative to the *new* direction of flow downstream of the expansion, namely, parallel to the upper wall of the wedge in Fig. 12–41 if we neglect the influence of the boundary layer along the wall. But how do we determine Ma_2? It turns out that the turning angle θ across the

expansion fan can be calculated by integration, making use of the isentropic flow relationships. For an ideal gas, the result is (Anderson, 2003),

Turning angle across an expansion fan: $$\theta = \nu(\mathrm{Ma}_2) - \nu(\mathrm{Ma}_1) \qquad \textbf{(12–48)}$$

where $\nu(\mathrm{Ma})$ is an angle called the **Prandtl–Meyer function** (not to be confused with the kinematic viscosity),

$$\nu(\mathrm{Ma}) = \sqrt{\frac{k+1}{k-1}}\tan^{-1}\left(\sqrt{\frac{k-1}{k+1}(\mathrm{Ma}^2-1)}\right) - \tan^{-1}\left(\sqrt{\mathrm{Ma}^2-1}\right) \qquad \textbf{(12–49)}$$

Note that $\nu(\mathrm{Ma})$ is an angle, and can be calculated in either degrees or radians. Physically, $\nu(\mathrm{Ma})$ is the angle through which the flow must expand, starting with $\nu = 0$ at $\mathrm{Ma} = 1$, in order to reach a supersonic Mach number, $\mathrm{Ma} > 1$.

To find Ma_2 for known values of Ma_1, k, and θ, we calculate $\nu(\mathrm{Ma}_1)$ from Eq. 12–49, $\nu(\mathrm{Ma}_2)$ from Eq. 12–48, and then Ma_2 from Eq. 12–49, noting that the last step involves solving an implicit equation for Ma_2. Since there is no heat transfer or work, and the flow can be approximated as isentropic through the expansion, T_0 and P_0 remain constant, and we use the isentropic flow relations derived previously to calculate other flow properties downstream of the expansion, such as T_2, ρ_2, and P_2.

Prandtl–Meyer expansion fans also occur in axisymmetric supersonic flows, as in the corners and trailing edges of a cone-cylinder (Fig. 12–42). Some very complex and, to some of us, beautiful interactions involving both shock waves and expansion waves occur in the supersonic jet produced by an "overexpanded" nozzle, as in Fig. 12–43. When such patterns are visible in the exhaust of a jet engine, pilots refer to it as a "tiger tail." Analysis of such flows is beyond the scope of the present text; interested readers are referred to compressible flow textbooks such as Thompson (1972), Leipmann and Roshko (2001), and Anderson (2003).

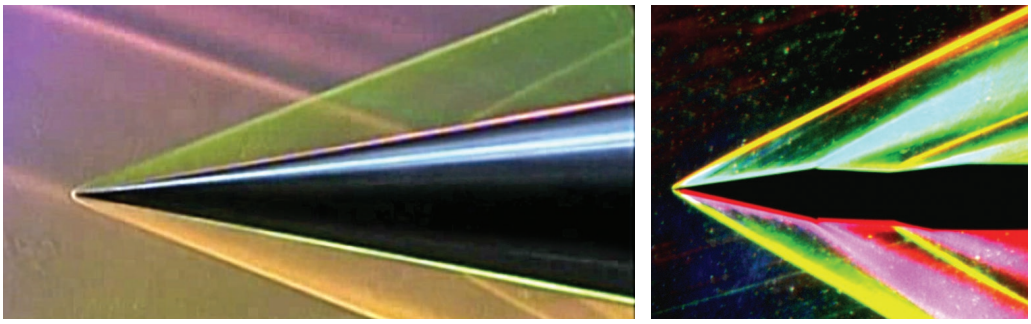

(*a*) (*b*)

FIGURE 12–42

(*a*) Mach 3 flow over an axisymmetric cone of 10-degree half-angle. The boundary layer becomes turbulent shortly downstream of the nose, generating Mach waves that are visible in the color schlieren image. (*b*) A similar pattern is seen in this color schlieren image for Mach 3 flow over an 11-degree 2-D wedge. Expansion waves are seen at the corners where the wedge flattens out.

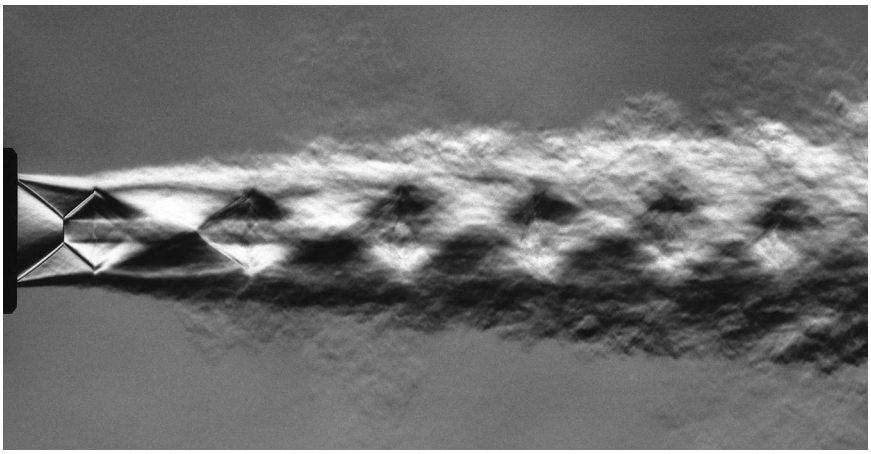

(*a*)

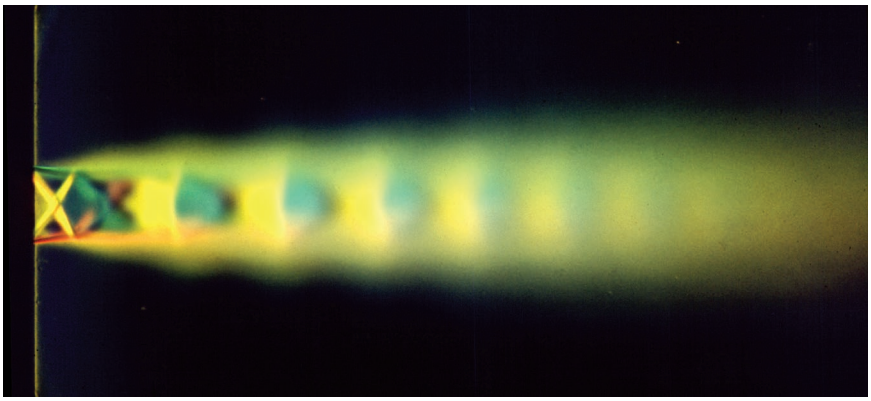

(*b*)

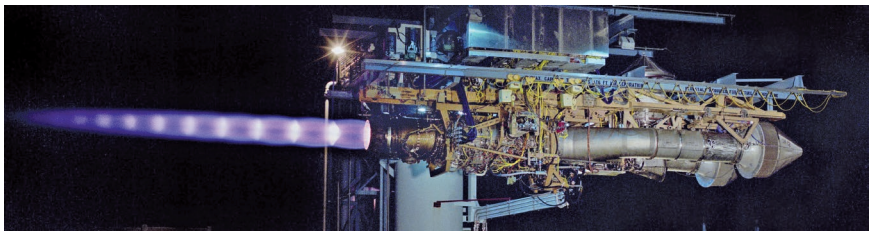

(*c*)

FIGURE 12–43
The complex interactions between shock waves and expansion waves in an "overexpanded" supersonic jet. (*a*) The flow is visualized by a schlieren-like differential interferogram. (*b*) Color shlieren image. (*c*) Tiger tail shock pattern.

(*a*) *Reproduced courtesy of the French-German Research Institute of Saint Louis, ISL.* (*b*) *© G.S. Settles, Gas Dynamics Lab, Penn State University. Used with permission.* (*c*) *Photo Courtesy Joint Strike Fighter Program, Department of Defense and Pratt & Whitney.*

EXAMPLE 12–9 **Estimation of the Mach Number from Mach Lines**

Estimate the Mach number of the free-stream flow upstream of the space shuttle in Fig. 12–32 from the figure alone. Compare with the known value of Mach number provided in the figure caption.

SOLUTION We are to estimate the Mach number from a figure and compare it to the known value.

Analysis Using a protractor, we measure the angle of the Mach lines in the free-stream flow: $\mu \cong 19°$. The Mach number is obtained from Eq. 12–47,

$$\mu = \sin^{-1}\left(\frac{1}{\text{Ma}_1}\right) \rightarrow \text{Ma}_1 = \frac{1}{\sin 19°} \rightarrow \text{Ma}_1 = \mathbf{3.07}$$

Our estimated Mach number agrees with the experimental value of 3.0 ± 0.1.

Discussion The result is independent of the fluid properties.

EXAMPLE 12–10 Oblique Shock Calculations

Supersonic air at $\text{Ma}_1 = 2.0$ and 75.0 kPa impinges on a two-dimensional wedge of half-angle $\delta = 10°$ (Fig. 12–44). Calculate the two possible oblique shock angles, β_{weak} and β_{strong}, that could be formed by this wedge. For each case, calculate the pressure and Mach number downstream of the oblique shock, compare, and discuss.

SOLUTION We are to calculate the shock angle, Mach number, and pressure downstream of the weak and strong oblique shock formed by a two-dimensional wedge.

Assumptions **1** The flow is steady. **2** The boundary layer on the wedge is very thin.

Properties The fluid is air with $k = 1.4$.

Analysis Because of assumption 2, we approximate the oblique shock deflection angle as equal to the wedge half-angle, i.e., $\theta \cong \delta = 10°$. With $\text{Ma}_1 = 2.0$ and $\theta = 10°$, we solve Eq. 12–46 for the two possible values of oblique shock angle β: $\beta_{\text{weak}} = \mathbf{39.3°}$ and $\beta_{\text{strong}} = \mathbf{83.7°}$. From these values, we use the first part of Eq. 12–44 to calculate upstream normal Mach number $\text{Ma}_{1,n}$,

Weak shock: $$\text{Ma}_{1,n} = \text{Ma}_1 \sin\beta \rightarrow \text{Ma}_{1,n} = 2.0 \sin 39.3° = 1.267$$

and

Strong shock: $$\text{Ma}_{1,n} = \text{Ma}_1 \sin\beta \rightarrow \text{Ma}_{1,n} = 2.0 \sin 83.7° = 1.988$$

We substitute these values of $\text{Ma}_{1,n}$ into the second equation of Fig. 12–36 to calculate the downstream normal Mach number $\text{Ma}_{2,n}$. For the weak shock, $\text{Ma}_{2,n} = 0.8032$, and for the strong shock, $\text{Ma}_{2,n} = 0.5794$. We also calculate the downstream pressure for each case, using the third equation of Fig. 12–36, which gives

Weak shock:

$$\frac{P_2}{P_1} = \frac{2k\,\text{Ma}_{1,n}^2 - k + 1}{k+1} \rightarrow P_2 = (75.0\text{ kPa})\frac{2(1.4)(1.267)^2 - 1.4 + 1}{1.4 + 1} = \mathbf{128\text{ kPa}}$$

and

Strong shock:

$$\frac{P_2}{P_1} = \frac{2k\,\text{Ma}_{1,n}^2 - k + 1}{k+1} \rightarrow P_2 = (75.0\text{ kPa})\frac{2(1.4)(1.988)^2 - 1.4 + 1}{1.4 + 1} = \mathbf{333\text{ kPa}}$$

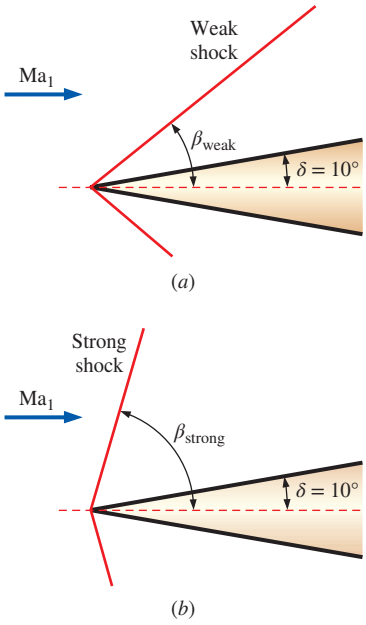

FIGURE 12–44
Two possible oblique shock angles, (*a*) β_{weak} and (*b*) β_{strong}, formed by a two-dimensional wedge of half-angle $\delta = 10°$.

Finally, we use the second part of Eq. 12–44 to calculate the downstream Mach number,

Weak shock:
$$\mathrm{Ma}_2 = \frac{\mathrm{Ma}_{2,n}}{\sin(\beta - \theta)} = \frac{0.8032}{\sin(39.3^\circ - 10^\circ)} = \mathbf{1.64}$$

and

Strong shock:
$$\mathrm{Ma}_2 = \frac{\mathrm{Ma}_{2,n}}{\sin(\beta - \theta)} = \frac{0.5794}{\sin(83.7^\circ - 10^\circ)} = \mathbf{0.604}$$

The changes in Mach number and pressure across the strong shock are much greater than the changes across the weak shock, as expected.

Discussion Since Eq. 12–46 is implicit in β, we solve it by an iterative approach or with an equation solver. For both the weak and strong oblique shock cases, $\mathrm{Ma}_{1,n}$ is supersonic and $\mathrm{Ma}_{2,n}$ is subsonic. However, Ma_2 is *supersonic* across the weak oblique shock, but *subsonic* across the strong oblique shock. We could also use the normal shock tables in place of the equations, but with loss of precision.

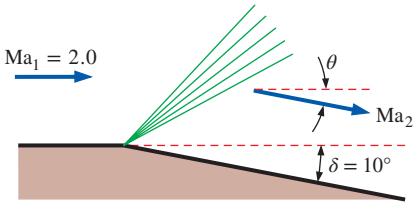

FIGURE 12–45
An expansion fan caused by the sudden expansion of a wall with $\delta = 10^\circ$.

EXAMPLE 12–11 Prandtl–Meyer Expansion Wave Calculations

Supersonic air at $\mathrm{Ma}_1 = 2.0$ and 230 kPa flows parallel to a flat wall that suddenly expands by $\delta = 10^\circ$ (Fig. 12–45). Ignoring any effects caused by the boundary layer along the wall, calculate downstream Mach number Ma_2 and pressure P_2.

SOLUTION We are to calculate the Mach number and pressure downstream of a sudden expansion along a wall.

Assumptions **1** The flow is steady. **2** The boundary layer on the wall is very thin.

Properties The fluid is air with $k = 1.4$.

Analysis Because of assumption 2, we approximate the total deflection angle as equal to the wall expansion angle, i.e., $\theta \cong \delta = 10^\circ$. With $\mathrm{Ma}_1 = 2.0$, we solve Eq. 12–49 for the upstream Prandtl–Meyer function,

$$\nu(\mathrm{Ma}) = \sqrt{\frac{k+1}{k-1}}\tan^{-1}\left(\sqrt{\frac{k-1}{k+1}(\mathrm{Ma}^2 - 1)}\right) - \tan^{-1}\left(\sqrt{\mathrm{Ma}^2 - 1}\right)$$

$$= \sqrt{\frac{1.4+1}{1.4-1}}\tan^{-1}\left(\sqrt{\frac{1.4-1}{1.4+1}(2.0^2 - 1)}\right) - \tan^{-1}\left(\sqrt{2.0^2 - 1}\right) = 26.38^\circ$$

Next, we use Eq. 12–48 to calculate the downstream Prandtl–Meyer function,

$$\theta = \nu(\mathrm{Ma}_2) - \nu(\mathrm{Ma}_1) \;\rightarrow\; \nu(\mathrm{Ma}_2) = \theta + \nu(\mathrm{Ma}_1) = 10^\circ + 26.38^\circ = 36.38^\circ$$

Ma_2 is found by solving Eq. 12–49, which is implicit—an equation solver is helpful. We get $\mathrm{Ma}_2 = \mathbf{2.38}$. There are also compressible flow calculators on the Internet that solve these implicit equations, along with both normal and oblique shock equations; e.g., see www.aoe.vt.edu/~devenpor/aoe3114/calc.html.

We use the isentropic relations to calculate the downstream pressure,

$$P_2 = \frac{P_2/P_0}{P_1/P_0} P_1 = \frac{\left[1 + \left(\frac{k-1}{2}\right)\text{Ma}_2^2\right]^{-k/(k-1)}}{\left[1 + \left(\frac{k-1}{2}\right)\text{Ma}_1^2\right]^{-k/(k-1)}} (230 \text{ kPa}) = \mathbf{126 \text{ kPa}}$$

Since this is an expansion, Mach number increases and pressure decreases, as expected.

Discussion We could also solve for downstream temperature, density, etc., using the appropriate isentropic relations.

12–5 ▪ DUCT FLOW WITH HEAT TRANSFER AND NEGLIGIBLE FRICTION (RAYLEIGH FLOW)

So far we have limited our consideration mostly to *isentropic flow,* also *called reversible adiabatic flow* since it involves no heat transfer and no irreversibilities such as friction. Many compressible flow problems encountered in practice involve chemical reactions such as combustion, nuclear reactions, evaporation, and condensation as well as heat gain or heat loss through the duct wall. Such problems are difficult to analyze exactly since they may involve significant changes in chemical composition during flow, and the conversion of latent, chemical, and nuclear energies to thermal energy (Fig. 12–46).

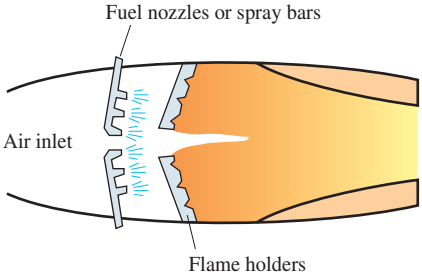

FIGURE 12–46
Many practical compressible flow problems involve combustion, which may be modeled as heat gain through the duct wall.

The essential features of such complex flows can still be captured by a simple analysis by modeling the generation or absorption of thermal energy as heat transfer through the duct wall at the same rate and disregarding any changes in chemical composition. This simplified problem is still too complicated for an elementary treatment of the topic since the flow may involve friction, variations in duct area, and multidimensional effects. In this section, we limit our consideration to one-dimensional flow in a duct of constant cross-sectional area with negligible frictional effects.

Consider steady one-dimensional flow of an ideal gas with constant specific heats through a constant-area duct with heat transfer, but with negligible friction. Such flows are referred to as **Rayleigh flows** after Lord Rayleigh (1842–1919). The conservation of mass, momentum, and energy equations for the control volume shown in Fig. 12–47 are written as follows:

Continuity equation Noting that the duct cross-sectional area A is constant, the relation $\dot{m}_1 = \dot{m}_2$ or $\rho_1 A_1 V_1 = \rho_2 A_2 V_2$ reduces to

$$\rho_1 V_1 = \rho_2 V_2 \qquad \textbf{(12–50)}$$

***x*-Momentum equation** Noting that the frictional effects are negligible and thus there are no shear forces, and assuming there are no external and body forces, the momentum equation $\sum \vec{F} = \sum_{\text{out}} \beta \dot{m} \vec{V} - \sum_{\text{in}} \beta \dot{m} \vec{V}$

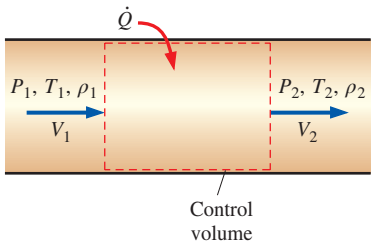

FIGURE 12–47
Control volume for flow in a constant-area duct with heat transfer and negligible friction.